Geomorphology 226 (2014) 106–123

Contents lists available at ScienceDirect

Geomorphology

journal homepage: www.elsevier.com/locate/geomorph

Structural and lithological guidance on speleogenesis in quartz–sandstone: Evidence of the arenisation process

Francesco Sauro *

Dipartimento di Scienze Biologiche, Geologiche e Ambientali, Italian Institute of Speleology, Via Zamboni 67, 40126 Bologna, Italy
La Venta Esplorazioni Geografiche Association, Via Priamo Tron 35/F, 31100 Treviso, Italy

ARTICLE INFO

Article history:
Received 22 April 2014
Received in revised form 31 July 2014
Accepted 31 July 2014
Available online 9 August 2014

Keywords:
Speleogenesis
Weathering
Strata-bounded fractures
Arenisation
Tepui
Venezuela

ABSTRACT

A detailed petrographic, structural and morphometric investigation of different types of caves carved in the quartz–sandstones of the "tepui" table mountains in Venezuela has allowed identification of the main speleogenetic factors guiding cave pattern development and the formation of particular features commonly found in these caves, such as funnel-shaped pillars, pendants and floor bumps. Samples of fresh and weathered quartz–sandstone of the Mataui Formation (Roraima Supergroup) were characterised through WDS dispersive X-ray chemical analyses, picnometer measurements, EDAX analyses, SEM and thin-section microscopy. In all the caves two compositionally different strata were identified: almost pure quartz–sandstones, with content of silica over 95% and high primary porosity (around 4%), and phyllosilicate-rich quartz–sandstone, with contents of aluminium over 10% and low primary porosity (lower than 0.5%). Phyllosilicates are mainly pyrophyllite and kaolinite. SEM images on weathered samples showed clear evidence of dissolution on quartz grains to different degrees of development, depending on the alteration state of the samples. Grain boundary dissolution increases the rock porosity and gradually releases the quartz grains, suggesting that arenisation is a widespread and effective weathering process in these caves. The primary porosity and the degree of fracturing of the quartz–sandstone beds are the main factors controlling the intensity and distribution of the arenisation process. Weathering along iron hydroxide or silt layers, which represent inception horizons, or a strata-bounded fracture network, predisposes the formation of horizontal caves in specific stratigraphic positions. The loose sands produced by arenisation are removed by piping processes, gradually creating anastomosing open-fracture systems and forming braided mazes, geometric networks or main conduit patterns, depending on the local lithological and structural guidance on the weathering process. This study demonstrates that all the typical morphologies documented in these quartz–sandstone caves can be explained as a result of arenisation, which is guided by layers with particular petrographic characteristics (primary porosity, content of phyllosilicates and iron hydroxides), and different degrees of fracturing (strata-bounded fractures or continuous dilational joints).

1. Introduction

About thirty years ago cavers and karst scientists believed that speleogenesis of caves in quartz–sandstones was related to exceptional conditions and only of local importance because of the extremely low solubility and dissolution rate of quartz (Tricart, 1972; Wray, 1993, 1997a, 2013). Since 2000, several huge horizontal cave systems have been explored in the "tepui" table mountains of Venezuela (Fig. 1), showing a wide variety of morphologies and dimensions that compare well with the most developed cave systems in classic carbonate karst (Aubrecht et al., 2012; Sauro et al., 2013b).

This paradox of widespread, complex and km-long cave systems in one of the hardest and least soluble rocks on Earth obviously requires us to rediscuss the speleogenetic processes responsible for their formation. Until now, most of the theories so far presented involve the formation of loose sands along some preferential bedding planes or fractures and their winnowing-out (piping) by underground flowing waters (Szczerban and Urbani, 1974; Galán and Lagarde, 1988). The role in generating the "loose sands" has been assigned to rock dissolution by meteoric (Jennings, 1983; Martini, 2000; Wray, 2000; Piccini and Mecchia, 2009; Mecchia et al., 2014) or hydrothermal waters (Zawidzki et al., 1976; Sauro et al., 2014) through a weathering dissolution process called "arenisation". Other authors assign importance to microbially-driven alkaline dissolution (Marker, 1976; Barton et al., 2009) or refer to the existence of unlithified beds (Aubrecht et al., 2008, 2011, 2012). All these theories are still under discussion and there is not yet a clear understanding of the main speleogenetic and morphogenetic processes involved. Sauro et al. (2013b, 2013c) suggested that quartz–sandstone could be weathered according to the "arenisation" model (Martini, 2000) and that the degree of fracturing, the mineralogical composition

* Dipartimento di Scienze Biologiche, Geologiche e Ambientali, Italian Institute of Speleology, Via Zamboni 67, 40126, Bologna, Italy.
E-mail address: cescosauro@gmail.com.

http://dx.doi.org/10.1016/j.geomorph.2014.07.033
0169-555X/

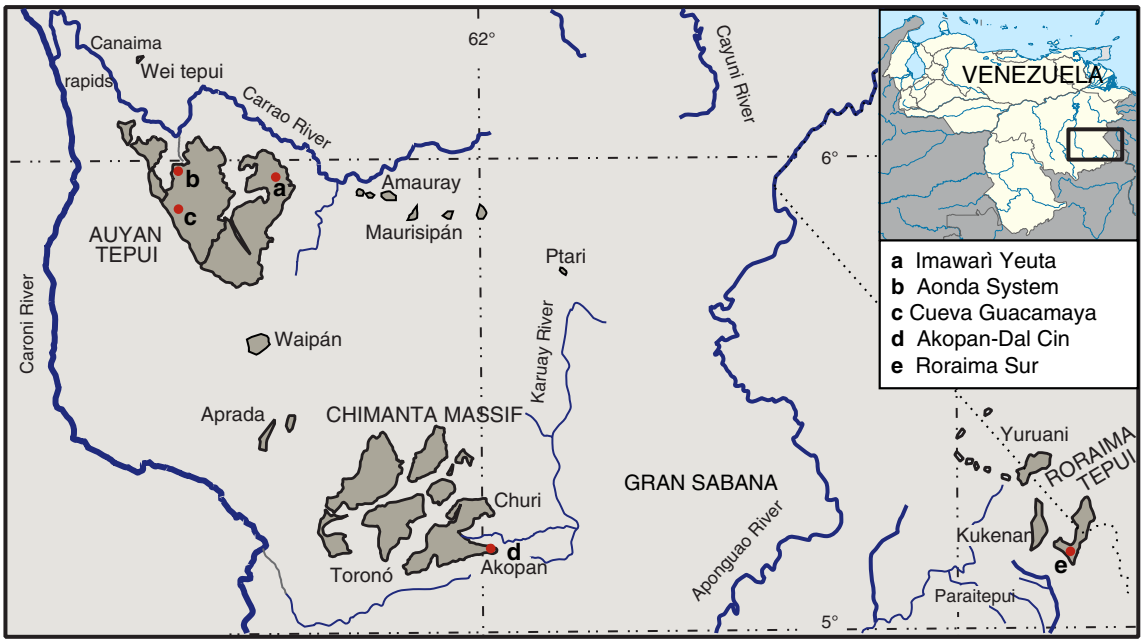

Fig. 1. Geographic location of tepui massifs in the Gran Sabana region and the investigated cave systems. In Auyan Tepui: Imawarì Yeuta, Guacamaya cave, Aonda and Auyantepuy Noroeste systems. In the Chimanta massif: Akopan-Dal Cin System. In the Roriama Tepui: Roraima Sur System.

and the petrographical features (grain size, sorting, depositional structures, primary porosity), and not the diagenetic degree of the quartz–sandstone as suggested by Aubrecht et al. (2011), probably control the intensity of the weathering processes along the strata.

The main discussion has focused on the presence of some typical morphologies, like funnel-shaped pillars and pendants. These features are considered by Aubrecht et al. (2013) as channels of a descending silica-bearing hardening diagenetic fluid flow, while for Sauro et al. (2013b) they represent secondary forms due to arenisation and erosion processes along fracture networks.

Kilometre-long caves in the Roraima and Chimanta massifs have been explored by Venezuelan, Czech and Slovak speleologists since 2003 (Fig. 2; Galán et al., 2004; Aubrecht et al., 2012; Audy and Bouda, 2013). In April 2013 a new giant cave was discovered by a joint Italian–Venezuelan expedition on the Auyan Tepui in the Canaima National Park. The system was named Imawarì Yeuta (the "Cave where the Gods live" in Pemon Kamarakoto native language), and reaches now 20 km of development, being actually the longest quartzite cave in the world (Sauro et al., 2013b). Besides its dimensions (Figs. 1, 2a), the scientific interest of this cave is very high, and all the characteristic formations described by Aubrecht et al. (2011, 2012) for the quartz–sandstone caves of the Churì Tepui and Roraima are well represented. During two expeditions in March 2013 and March 2014, detailed morphometric studies were performed, together with a

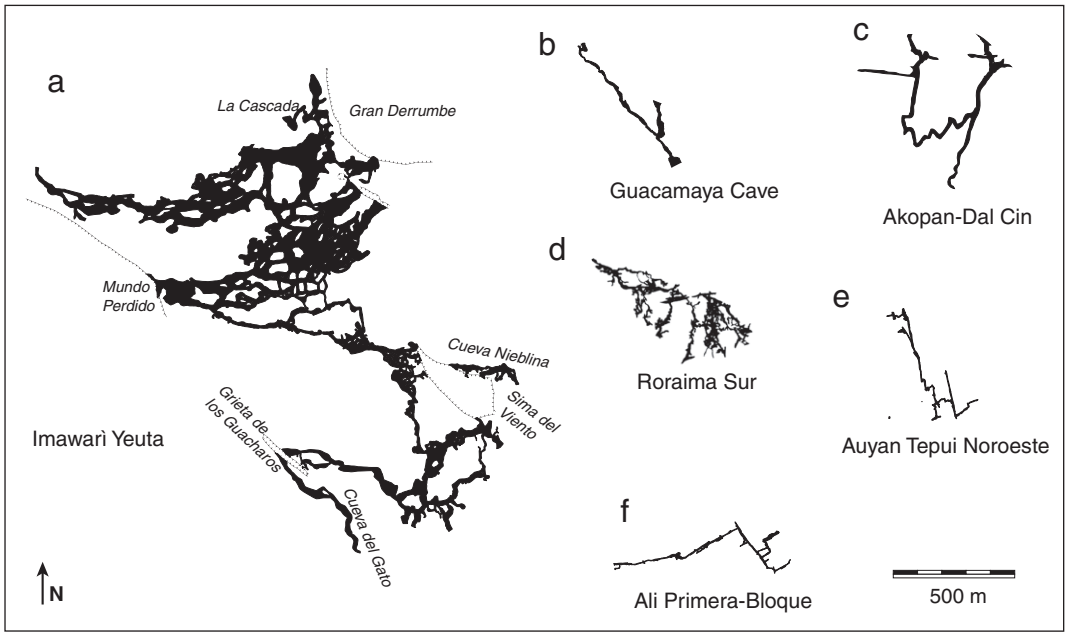

Fig. 2. Plan view and size/pattern comparison of the investigated cave systems. The survey of Roraima Sur is adapted from Aubrecht et al. (2013), all the others are from the La Venta Archive.

detailed survey and sampling of weathered and unweathered quartz–sandstones. The data from Imawarì Yeuta were then compared with further morphological observations and sample analyses from other caves developed in the Mataui Formation: the Roraima Sur System in the Roraima Tepui (Galán et al., 2004; Aubrecht et al., 2012), the Akopan-Dal Cin System in the Chimanta massif (Mecchia et al., 2009; Sauro, 2009), Guacamaya cave in the western sector of Auyan Tepui (Sauro et al., 2013d) and the deep crevice networks of the Aonda and Auyan Tepui Noroeste systems (Piccini and Mecchia, 2009).

The aim of this research is to identify the main factors guiding the formation of caves along specific layers and to explain the processes responsible for the formation of pillars and other similar morphologies. In order to do this, the following methods were used: 1) mineralogical, chemical and petrographical analysis of the quartz–sandstone beds; 2) SEM imaging in order to identify dissolution morphologies on the quartz grains and other potential weathering processes; and 3) morphometric measurements and statistics of quartz–sandstone pillars in the Imawarì Yeuta cave in order to explain their relationship with fracture sets and the degree of fracturing.

2. Regional setting

The Gran Sabana is a vast geographical region, part of the Guyana Shield, located in northern South America, between Venezuela and Brazil, crossed by several tributaries of the Rio Caroní, which in turn flows into the Orinoco River (Fig. 1). The main massifs of the Gran Sabana have the shape of large table mountains named "tepuis", which means "house of the Gods" or simply "mountain" in the local indigenous Pemón language. The tepuis are delimited by vertical to overhanging cliffs many hundreds of metres high which divide the massifs from each other. The mountains are surrounded by the lowlands of the Wonkén planation surface (Briceño and Schubert, 1990). The summit plateaus consist of a series of stratigraphically controlled planar surfaces (in general grouped into the Auyan planation surface, between 2000 and 2900 m a.s.l., considered of Mesozoic age by Briceño and Schubert (1990)) divided by secondary scarps. More than 60 tepuis occur in the Gran Sabana region but our research focused on the most important massifs (Fig. 1): 1) Auyan Tepui (700 km^2), one of the largest of the area, famous for the Angel Fall that is considered the highest waterfall in the world with 975 m of vertical drop, 2) Roraima Tepui (31 km^2) and 3) Akopan Tepui, in the southeastern sector of the Chimanta massif (composed of different tepuis with a total surface of 1470 km^2).

The igneous and metamorphic rocks in the northern portion of the Guyana Shield (Imataca-Bolivar Province, after González de Juana et al. (1980)) have an age of 3.5 Ga. The siliciclastic rocks of the Roraima Group belong to the continental and pericontinental environment of the Roraima-Canaima Province (Reid, 1974). The age of this arenaceous group can be inferred only on the basis of the absolute dating of the granitic basement (2.3–1.8 Ga) and of the basaltic dykes and sills that cross the upper formation of the Roraima Group (1.4–1.8 Ga) (Briceño and Schubert, 1990; Santos et al., 2003). The Roraima Group was also intruded by Mesozoic basalts forming thin NE-trending dykes with ages of around 200 Ma (Hawkes, 1966; Teggin et al., 1985). A low-grade metamorphic overprint, leading to quartz grain overgrowths and pyrophyllite–muscovite formation in the more pelitic beds, is the result of the lithostatic load of ~3-km thick sediments which are now eroded (Urbani et al., 1977).

Caves are developed in the Mataui Formation, the youngest, presently outcropping sedimentary unit of the Roraima Group. This formation is 600–900 m thick and ~1.5 Ga old, and represents the bordering walls and the summit part of the tepuis (Santos et al., 2003). Quartz commonly represents over 90% of the rock, giving the name "quartz–sandstone" (Martini, 2000, 2004). The quartz grains are well-sorted, usually between 30 and 200 μm in diameter, and cemented by syntaxial quartz overgrowths or by minor pore-filling phyllosilicates (pyrophyllite and/or kaolinite). The slopes at the foot of the cliffs surrounding the tepuis are made of proto-quartzites, arkoses and graywackes, with beds of cherts, lutites and siltites (Uaimapué Formation; Reid, 1974). In the lowlands the main outcropping lithology is the Kukenán Formation, composed mainly of siltites and shales.

From a structural point of view, the bedding is normally horizontal, locally slightly inclined. Sets of mainly vertical fractures cut the plateaus, creating a regular network of quadrangular or rhomboidal prisms. Important regional faults with significant displacement have not been observed in the Gran Sabana area (Gibbs and Barron, 1993).

All the examined tepuis exhibit a similar morphology: 1) a slightly inclined pediment formed by detrital talus on the more erodible lithologies of the Uaimapué Formation; 2) an external vertical cliff (Mataui Formation), up to 1 km high, presenting a few major benches in specific stratigraphic positions; and 3) an upper plateau divided in at least two secondary platforms with about 100–150 m of altitude difference, controlled by specific stratigraphic layers. The lower platform is usually characterised by extensive fields of collapsed boulders, while the higher platform is more regular and flat without rock-piles, but often presenting wide fields of towers, crevices and "rock cities".

The average annual rainfall is 3400–3600 mm. The average daily temperature is fairly constant all year round, with an estimated 13.9 °C at 2200 m altitude, and a mean difference between day and night of 10 °C (Galán, 1992).

The high rainfall supports a temperate vegetation; forests, sedges, grasses, and bromeliads grow in the sheltered locations, peat swamps and bogs are well-developed and often extensive, particularly where the substrate is characterised by weathered diabase sills (Briceño and Schubert, 1990). Quartz–sandstone outcrops are bare of vegetation except for mosses, lichens and algae. The water flows on the plateaus and forms high waterfalls along the external cliffs, or sinks in fractures and cave systems to later resurge from springs scattered around the cliffs (Mecchia and Piccini, 1999).

3. The caves

3.1. The Imawarì Yeuta cave system

The Imawarì Yeuta System is situated in the northeastern sector of the Auyan Tepui at a mean altitude of 1980 m a.s.l. (Fig. 1a) and consists of three genetically related caves (Cueva Imawarì, 18.7 km; Cueva de la Nieblina; 0.65 km; Cueva del Gato, 0.65 km; Fig. 2a) presently dissected by collapses. All the cave conduits develop at the same stratigraphic elevation of the lower platform, extending about 100–150 m beneath the upper platform surface (Fig. 3a) (Sauro et al., 2013b). The main entrances to the system are situated at the base of the tepui internal cliff borders or at the bottom of deep giant collapse dolines (*simas*; like "Sima del Viento" and "Gran Derrumbe" in Figs. 2a–3a) and joint-controlled, elongated depressions (*grietas*; like Grieta de Los Guacharos in Figs. 2a–3a) opening in the inner part of the upper platform. The direction of drainage is in general from ENE to WSW, following the gentle dip of the quartz–sandstone beds.

From a hydrological point of view, the cave system consists of three independent collectors, two of them draining a big collapse doline named Sima del Viento and the northern sector of Cueva Nieblina, while the most important one derives from the catchment area of a larger circular collapse doline to the north (Gran Derrumbe, Figs. 2a–3a), about 500 m wide, and of a nearby smaller sinkhole (La Cascada; Fig. 3a). Here a stream falls into the cave from the upper platform through a c. 90-m high waterfall. During the expeditions, carried out during the dry season, the first two streams had a minimum discharge of about 20 l/s, while the main river reaches a minimum of 100 l/s. From the signs left by water on the walls it was evident that this last river can probably reach several thousands of litres per second during the rainy season, flooding the lower sectors of the cave. A labyrinth network of inactive galleries, developed along a distinctive stratigraphic position, interconnects the different rivers. The guiding stratum is

Fig. 3. Plan projection and typical morphologies of Imawarì Yeuta cave: a) projection of the cave map on the tepui surface: the cave develops at the height of the lower platform with the main entrances located in deep collapses, grietas or at the base of the cliff rims of the higher platform; b) hundred metres wide strata-bounded environments with flat ceilings characterise the cave system; c) conduits in the upper dry level of galleries of the system are characterised by rounded cross-sections that might be of phreatic origin; d) field of funnel-shaped pillars in the Galeria de las Mil Columnas, along one of the three main streams of the cave; and e) complex environments with bumps rising from the floor, pendants, pillar and septums characterise the Universo del Silencio sector of the cave.
Photos from Vittorio Crobu *and Fulvio Iorio*, La Venta Geographic Explorations Team.

situated some metres above the actual stream levels and, where preserved, is often characterised by the presence of a layer of iron hydroxides laminated with amorphous silica, resembling Banded Iron Formation described in other caves of the area (Guacamaya cave; Sauro et al., 2013d). The voids formed along this bed can reach impressive widths (more than 300 m in some sectors) creating huge flat environments where the ceiling is supported only by relict pillars and wide columns (Fig. 3b). This situation causes large collapse zones with a chaotic floor of fallen boulders and quartz–sandstone slabs. Some dry galleries situated some metres above the actual stream thalwegs show a rounded cross-section and are in general almost perpendicular to the present vadose drainage (Fig. 3c).

The most representative features characterising the cave system are layer-bounded pillars (Fig. 3d). These features are very similar to those described by Aubrecht et al. (2012) for the Churì and Roraima Tepui caves and by Doerr (1999) in the Kukenan Tepui, but with an even wider variety of forms and dimensions. Pillars are normally 1 to 3 m high, often characterised by elliptical cross-sections with the major axes from a few centimetres to several metres long. They develop only along specific strata, bounded by harder and more regular strata, and

always below the main iron-hydroxide guiding layer. Small pillars are characterised by a funnel shape with a vertical or, more often, slightly inclined axis and an elliptical rather than circular cross-section of the narrower central part up to 1 m in diameter. With increasing size the funnel shape is less prominent, becoming more cylindrical. In many cases the pillars have an elongated form in plan view, sometimes becoming a true septum dividing the cave passages in parallel corridors. At even greater size (more than 5 m in diameter) they constitute rough massive columns sometimes surrounded by minor funnel-shaped pillars. These morphologies are not widespread in the cave, but they are concentrated in specific locations, mainly on the lateral side of hydrologically active galleries. Small funnel-shaped pillars are particularly well developed (in groups of more than forty pillars in only a few tens of metres) along the outer convex walls of meanders and in the lower, often partially flooded, levels of the river beds. Other related typical morphologies are elliptical or rhombohedral pendants protruding from the ceiling or similar bumps rising from the floor (Fig. 3e). Similar mammillary forms were also described by Aubrecht et al. (Fig. 2a–b in 2013) in the Muchimuk Cave System. Likewise to the pillars, these features can have different sizes, and they are concentrated only in specific sectors of the cave. In general the presence of pillars and septums of all sizes gives a general maze network to the cave, clearly recognisable in the topographic survey plan view (Fig. 2a).

The cave is also characterised by the presence of spectacular silica speleothems and gypsum formations, and by iron hydroxide (mainly goethite and limonite) forming brownish deposits on the floor. These goethite speleothems were described also in other quartzite caves of the Sarisariñama and Chimanta Tepuis (Zawidzki et al., 1976; Aubrecht et al., 2012).

3.2. The Guacamaya cave

Guacamaya cave represents the first horizontal cave discovered in Auyan Tepui in 2009 (Sauro, 2009; Sauro et al., 2013d; Fig. 1c). Different from Imawarì Yeuta, this cave system presents a “main conduit” pattern (Fig. 2b). The cave develops at the level of the lower platform, and in general the cave conduits are situated at shallow depth from the surface, only 30–50 m below the upper platform in some places. The total

Fig. 4. Typical cave morphologies from other investigated systems of the Gran Sabana tepuis: a) an active gallery in the Guacamaya cave with keyhole cross-section developed along a bed of iron-hydroxides (arrow); b) the BIF-like stratum guiding the galleries in the Guacamaya cave (arrow); c) entrance gallery of the Akopan cave with a rectangular cross-section guided by the intersection of an iron hydroxide layer and a major fracture (arrow on the ceiling); d) fracture-controlled vertical narrow canyon in the Ali Primera Resurgence in the Aonda system; and e) the Ojos de Cristal entrance in the Roraima Sur system: the cave is developed along a specific quartz–sandstone stratum while massive banks form overhanging ledges. Photo from Vittorio Crobu (a, b, c, e) and from Tullio Bernabei (d), La Venta Geographic Explorations Team.

development is 1.1 km. The main corridor is a hydrologic through-passage about 350 m long with a permanent stream of some litres per second crossing the cave from the sinkhole to the resurgence (Fig. 4a). About one hundred metres from the lower entrance, a lateral inactive branch develops straight to the south for 700 m ending in a boulder choke close to the surface. The passage is more than 30 m wide and about 15 m high in some sectors, with a great collapse room at the intersection of the two branches. Both the active and the dry branches are developed along a layer of iron hydroxides with minor amorphous silica, similar to Banded Iron Formations, from some decimetres to a metre thick (arrows in Fig. 4a–b). The cross-sections of the galleries show an elliptical or keyhole profile developed along this stratum (Sauro et al., 2013d). Original small rounded conduits entrenched by vadose canyons are recognisable. Pillars are very rare while only in the lower part of the hydrologically active tunnel, a few septums and bridges constituted by the hardest beds are recognisable in some sectors.

It is evident that the cave is part of a more extensive system, now dissected and open to the surface: the upstream and downstream valleys of the cave represent the unroofed continuation of the main conduit, following the same lithological layer.

3.3. The Akopan-Dal Cin cave system

Akopan-Dal Cin System is situated in the Akopan Tepui, in the southern sector of the Chimanta massif (Fig. 1d). This is a cave of more than 2.7 km in length (Fig. 2c), draining the higher plateau of the mountain through a large, 105-m deep collapsed doline (Mecchia et al., 2009). At the bottom of the doline the stream enters a horizontal meandering gallery, collecting waters from two other sinks. The river flows down to the lower entrance, called "Resurgencia Dal Cin", where the stream exits from the cave and forms a 200-m high waterfall on the external cliff. Just before the waterfall, a dry passage at the same level leads to another big entrance opening onto the external cliff, the Akopan cave (Fig. 4c).

In general, the cave passages present a rectangular cross-section of significant size, over 20 × 10 m (Fig. 4c). During floods these galleries can be completely flooded, as observed during an exceptional rain event in the expedition of February 2012. The main collector is a meandering passage following the gentle dip of the strata. The other branches, instead, are clearly controlled by vertical fractures and present a rectilinear development. Vertical and inclined pillars, forming peculiar rounded connection passages between parallel joints, are present only in the Tibia Rotta branch. These features were interpreted by Sauro et al. (2013c) as anastomosis of parallel vertical fractures (see Fig. 2 in Sauro et al., 2013c).

Also in the Akopan-Dal Cin System a unique stratum strictly controls the development of the conduits: all the passages follow a centimetre-thick quartz–sandstone bed characterised by millimetre-scale bands of iron hydroxides (Sauro et al., 2014). This level of horizontal conduits is situated at the same height of the major ledge characterising the external cliff of the Akopan Tepui.

3.4. The Roraima Sur cave system

The Roraima Sur cave system, known also as Ojos de Crystal cave system (Aubrecht et al., 2012), is a maze of low conduits developed at shallow depth from the surface, beneath the upper platform of the Roraima Tepui (Figs. 1e, 2d, 4e). Thin layers of siltstone and shale guide the whole cave where different collectors fed by sinking streams follow the gentle dip of the strata (Galán et al., 2004). The dimensions of the galleries are far smaller than the other horizontal caves described previously, rarely reaching more than 5 m width (Fig. 2d). The complex networks of galleries interconnected by narrow passages allowed surveying around 10 km of passages (Brewer-Carías and Audy, 2011). In general, the cave has an anastomotic pattern, with a few major collectors interconnected by dry side passages developed along the same strata. These conduits are characterised by non-excavated relicts of the strata in forms of flat columns. Funnel-shaped pillars are present only in a few parts of the cave and are in general less developed than those documented in Imawarì Yeuta. For a detailed description of the cave and the hydrological connections see Galán et al. (2004).

3.5. Fissure networks of the Aonda and Auyan Tepui Noroeste system

A different example of cave system in the quartz–sandstones of the Mataui Formation is given by the network collectors explored not only along the rims of the Aonda Canyon in the northwestern sector of the Auyan Tepui (Figs. 1–3; Sociedad Venezolana de Espeleologia, 1984; Bernabei et al., 1993; Gori et al., 1993; Rigamonti, 1995), but also close to the rims of other tepuis like Chimanta (Ipiña, 1994; Sociedad Venezolana de Espeleologia, 1994), Yuruani (Galán, 1991) and Wei Assipu (Carreño et al., 2002). The two most extensive systems are those of Auyan Tepui Noroeste (2.9 km of development, −370 m of depth; Fig. 2e) and the Ali Primera–Sima del Bloque cave stream network (2 km of development, −360 m of depth) resurging at the bottom of the deep Sima Aonda sinkhole (Figs. 1b, 2f). These systems consist of vertical shafts, up to about 200 m deep, developed along vertical fractures opened by gravitational release close to the tepui rims.

These caves are characterised by two different sectors: a mainly vertical part, consisting of deep shafts with only small ledges in specific stratigraphic positions, and a mainly horizontal and active network of passages developing around 300 m below the summit surface of the plateau. In plan view they have an angular pattern with elongated narrow corridors following the main fractures (Fig. 2e–f). The walls of the shafts are characterised by friable rock, commonly permanently wetted by percolation or condensation waters. Conversely, on the exposed outside cliff walls at the same stratigraphical height the rock is frequently very hard, suggesting that water derived from direct infiltration or condensation in the subsurface enhances the arenisation process responsible for weathering and consequent enlargement of the fracture walls (Piccini and Mecchia, 2009). At the bottom of the shafts, horizontal and high canyons direct the water toward the resurgences located along the external cliffs of the plateau. These conduits are developed mainly along the intersection between dilational fractures and specific stratigraphic levels, mainly siltstones and shale (Fig. 4d). In these collectors, peculiar features are represented by septums with rare aligned pillar morphologies separating parallel corridors.

4. Methods

4.1. Petrography, mineralogy and chemical composition

Petrographic studies on several quartz–sandstone samples from the Mataui Formation were carried out by means of transmitted light microscopy thin section observations, SEM imaging, EDAX chemical analyses of specific points, WD-XRF chemical bulk analyses, XRD mineral determinations, and porosity determination with gas displacement methods. Samples were collected in the Auyan, Akopan, Roraima Tepui, Aonda and Auyan Tepui Noroeste caves. Samples of pillars and massive banks with various degree of cohesion/hardness, fresh and weathered were collected in Imawarì Yeuta.

For SEM images a SEM Jeol JSM-5400 electron microscope at the BIGEA Department at the University of Bologna was used, digitalized with an iXRF 550i video card and equipped with a Si-drift detector for Energy Dispersive X-ray Spectroscopy.

For X-ray Diffraction analyses (XRD) quartz–sandstone samples were ground to an ultrafine powder in an agate mortar and lightly pressed in a plastic sample holder. XRD patterns were recorded with a Philips PW 1050/25 and a PANalytical X'Pert PRO diffractometer (experimental conditions 40 kV and 20 mA tube, CuKα Ni filtered

radiation λ = 1.5418 Å) at the Department of Chemical and Geological Sciences of Modena–Reggio Emilia University.

The bulk chemical determinations of 11 samples collected from cave walls in all the caves and from pillars in Imawarì Yeuta were obtained by two wave dispersive X-ray fluorescence spectrometers (WD-XRF) (PANalytical Axios, XRF Laboratory, BIGEA, Bologna, and PANalytical Axios at the Institute for Mineralogy and Petrology — IMP of ETH, Zurich) on pressed powder pellets, following the matrix correction methods of Franzini et al. (1972), Leoni and Saitta (1976) and Leoni et al. (1982). Calibration is based on 35 international reference materials. The estimated precision and accuracy for trace-element determinations are better than 5%, except for elements at <10 ppm (10–15%). Volatile content was evaluated by thermogravimetric TG–DTG–DTA analysis (XRF Laboratory, BIGEA, Bologna) in air atmosphere using a Setaram Labsys double-furnace apparatus (temperature range 20–1050 °C; heating rate 10 °C/min; platinum crucibles; calcined Al_2O_3 as reference substance; flow rate of air 0.27 ml/s; temperature accuracy about ±1 °C).

Porosity analyses on five dried cores collected in unweathered or slightly weathered quartz–sandstone samples from the Mataui Formation were performed at the Rock Deformation Lab of ETH (Zurich) with a helium picnometer (MicroMeritics-AccuPyc-1330), which measures the porosity by means of gas displacement and the sample volume/gas pressure relationship (Hartikainen et al., 1996).

4.2. Morphometric analyses

Morphometric measurements of 110 pillars were carried out in Imawarì Yeuta cave by means of a laser-distance meter Leica Disto D8 and the Cavesniper instrument (Megaplot SJ), a device equipped with an electronic compass integrated with a digital clinometer, whose readings are calculated with an ARM7TDMI processor. These instruments allowed rapid measurement, with a high degree of precision (accuracy respectively 1 mm and 1°), of the major (*M*) and minor axis (*m*) lengths of the central section, the direction (*D*) of the main axis, the dip (*i*) and dip direction (*id*) of the pillar (Fig. 5). Columns characterised by an ellipticity *e* (*M*/*m*) of the central part of the pillar higher than 3 and dimension of the major axis exceeding 1.5 m were avoided during the measurements because they were considered septums rather than proper pillars. In addition, in the surrounding area of every station we measured fractures and bedding plane dips and directions by means of a geological compass.

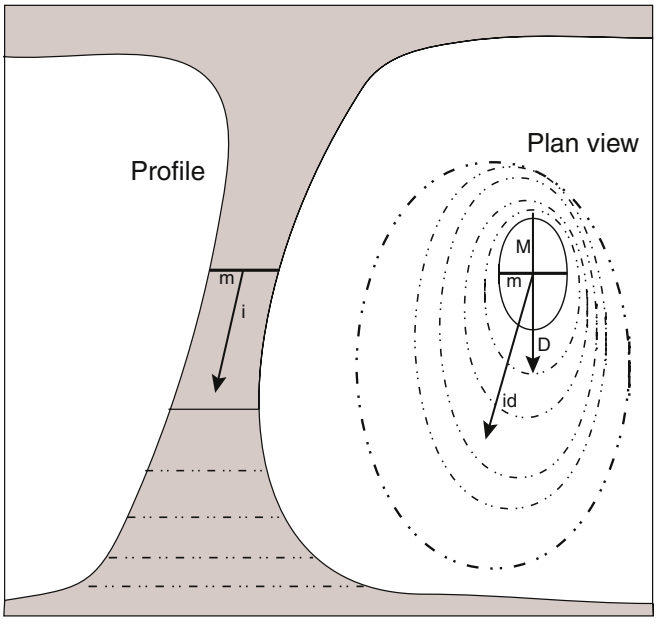

Fig. 5. Scheme showing the morphological measurements performed on the pillars in Imawarì Yeuta: minor axes (*m*), major axes (*M*), ellipse direction (*D*), pillar dip (*i*), and dip direction (*di*).

5. Results

5.1. Quartz–sandstone composition and petrography

In all the caves and in their surroundings two main lithologies can be clearly recognised by means of bulk compositional analyses (XRF): almost pure quartz–sandstone with silica content ranging between 95 and 99%, and aluminium phyllosilicate-rich quartz–sandstones with silica content around 70–90% and aluminium over 10–20% (Table 1).

From a petrographic point of view the almost pure quartz–sandstones are composed mainly of detrital monocrystalline quartz grains with non-undulatory extinction, disposed in interlocked structures due to the grain overgrowth during the burial metamorphism that evidently affected the Roraima Group (Urbani et al., 1977; Gibbs and Barron, 1993; Sauro et al., 2013b) (Fig. 6a). Conversely, in the second lithology phyllosilicates are abundant and constitute a pore-filling matrix (Fig. 6b). In some cases these phyllosilicates occur as a thin coating covering the interdigitated quartz grain rims (microstylolites), forming a typical texture of pressure solution during burial metamorphism (Sloss and Feray, 1948; Gratier et al., 2005; Fjellanger and Nystuen, 2007; Fig. 6c).

With increasing phyllosilicate content, the quartz grains show strong corrosion in contact with pyrophyllite due to the quartz-consuming *kaolinite + quartz = pyrophyllite* low grade metamorphic reaction (Hurst and Könkle, 1985) (Fig. 6d). In these matrix-rich samples pressure solution with grain overgrowth is evident only at the direct contact between quartz grains.

Opal-A and feldspars, suggested to be minor components of these lithologies by Aubrecht et al. (2011), were not observed in all our samples.

Phyllosilicates were characterised through XRD analyses as pyrophyllite ($A1_2Si_4O_{10}(OH)_2$), kaolinite ($Al_2Si_2O_5(OH)_4$), and rare muscovite ($KAl_2(AlSi_3O_{10})(F,OH)_2$). The first two minerals are the most abundant and can be easily distinguished also through SEM imaging and EDAX analyses of selected points (Fig. 7). Pyrophyllite appears as fan-shaped or needle-like masses radiating in various directions, filling pores between quartz grains. Chemical EDAX counts on these masses show the peak of aluminium almost at half-height of the silica peak because of the chemical ratio Si/Al = 2 in pyrophyllite. Conversely, kaolinite occurs in the form of microscopic pseudo-hexagonal plates and clusters of plates covering quartz grains, often growing on pyrophyllite masses. On kaolinite, the EDAX counts of aluminium are almost the same of silica because of the chemical ratio Si/Al = 1. Thus, the formation of the present phyllosilicate minerals can be ascribed to diagenetic mineral transformations in a more or less chemically closed system during the burial stage of the quartz–sandstone, or alternatively to subsequent weathering processes. What is evident at a first glance is that, in general, pyrophillite appears to be more abundant in fresh unweathered samples, while kaolinite is more common in weathered low cohesive ones.

The aluminium phyllosilicate-rich sandstone constitutes the hardest and most massive beds, with a glassy appearance and a conchoidal fracture in fresh samples, while the almost pure quartz–sandstone represents often the more weathered and low-cohesive strata, showing an earthier fracturing. The pillars were mainly developed in this latter lithology.

The picnometer measurements performed on fresh unweathered samples (Table 2) show a primary porosity one order of magnitude higher in almost pure quartz–sandstone with respect to the aluminium phyllosilicate-rich ones. The primary porosity is also controlled by

Table 1
Wavelength dispersive X-ray chemical analyses of different quartz–sandstone samples.

%	Sample	SiO_2	TiO_2	Al_2O_3	Fe_2O_3	MnO	MgO	CaO	Na_2O	K_2O	P_2O_5
Almost pure quartz – sandstones	AKT	96.03	0.05	3.28	0.10	0.001	0.005	0.017	0.419	0.059	0.015
	AK4	95.55	0.10	3.34	0.55	0.002	0.003	0.012	0.356	0.039	0.035
	R1	96.39	0.07	2.27	0.43	0.001	0.003	0.016	0.575	0.201	0.016
	V17	98.9	0.07	0.62	0.15	0.05	0.01	0.05	0	0.13	0.02
	V18	96.48	0.09	2.58	0.22	0.05	0.33	0.17	0.01	0.04	0.03
	V19	98.83	0.08	0.66	0.14	0.05	0.01	0.05	0	0.14	0.02
Aluminium phyllosilicate rich quartz – sandstone	AK5A	73.85	0.51	22.59	2.01	0.021	0.012	1.011	0.428	0.460	0.105
	AK5B	71.71	0.65	22.60	3.70	0.035	0.070	1.010	0.505	0.629	0.079
	AK5C	85.00	0.07	14.21	0.17	0.004	1.085	1.085	0.297	0.158	0.072
	AK3A	81.03	0.48	16.38	1.75	0.014	1.024	1.024	0.253	0.047	0.039
	ROR16	90.97	0.12	8.21	0.15	0.001	1.160	0.009	0.331	0.111	0.080

anisotropies, like parallel- and cross-bedding, varying in dependence of their orientation.

5.2. Evidence of the arenisation weathering process

SEM imaging was performed on seven quartz–sandstone samples collected in the caves. Samples collected from roofs, floors and from the inner part of funnel-shaped pillars are characterised by different cohesiveness. Despite some authors reported the absence of evident dissolution morphologies on samples collected from the Roraima Sur and Muchimuk cave systems (the latter in the Chimanta massif; Aubrecht et al., 2011, 2012, 2013), in our case most of the samples from all the investigated caves showed clear evidence of dissolution, with characteristic features at different degrees of development (Fig. 8). These findings are in agreement with the previous studies of Chalcraft and Pye (1984) and Ghosh (1985) on samples collected on the Roraima Tepui and with geochemical analyses of dissolved silica concentrations in drip waters in the investigated caves (Mecchia et al., 2014). The more cohesive samples show abundant welding between the grains by a pervasive syntaxial quartz overgrowth, but on the contrary the weathered, less cohesive samples show a wide network of voids between the grains. In these last samples, the surfaces of the quartz grains are also characterised by pervasive solutional pitting (Fig. 8a, b, c). In most of these cases dissolution along the quartz grains/overgrowths appears to be "surface controlled" (Burley and Kantorowicz, 1986) producing features typical of slow kinetics, such as well-defined, v-shaped pits (Fig. 8c). Dissolution is more active at high energy sites like face edges, corners and triple junctions of the quartz overgrowths (White and Peterson, 1990), gradually releasing the grain contacts (Fig. 8d–e).

Dissolution features are more evident in the almost pure quartz–sandstone than in the aluminium-phyllosilicate-rich ones. However they are often present also on quartz grains partially covered by kaolinite. Another process that affects the cohesiveness of the rock is the neoformation of kaolinite (Fig. 9). This happens through the dissolution–recrystallization reaction involving the metastable pyrophyllite in the presence of water, as described by Hurst and Könkle (1985). The neoformation is easily recognisable in the phyllosilicate-rich quartz–sandstone samples, suggesting that the majority of the kaolinite can be formed in subsurface conditions. Very similar processes

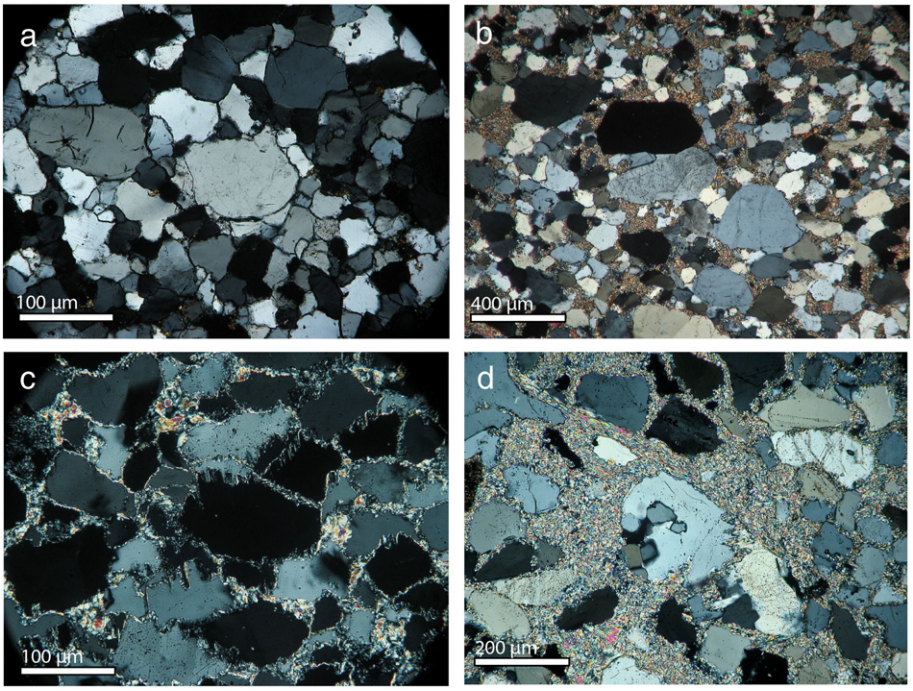

Fig. 6. Thin sections (at crossed nicols) of different unweathered quartz–sandstone samples: a) almost pure quartz–sandstone composed of quartz grains cemented by syntaxial overgrowths; b) quartz–sandstone characterised by a phyllosilicate matrix filling with evident overgrowths only at the direct contact between quartz grains; c) a thin coating of phyllosilicates (pyrophyllite) covers interdigitated quartz grains (microstylolites) typical of pressure solution during burial metamorphism; and d) in presence of high pyrophyllite content, the quartz grains are corroded by the quartz–consuming kaolinite + quartz = pyrophyllite low grade metamorphic reaction (Hurst and Könkle, 1985).

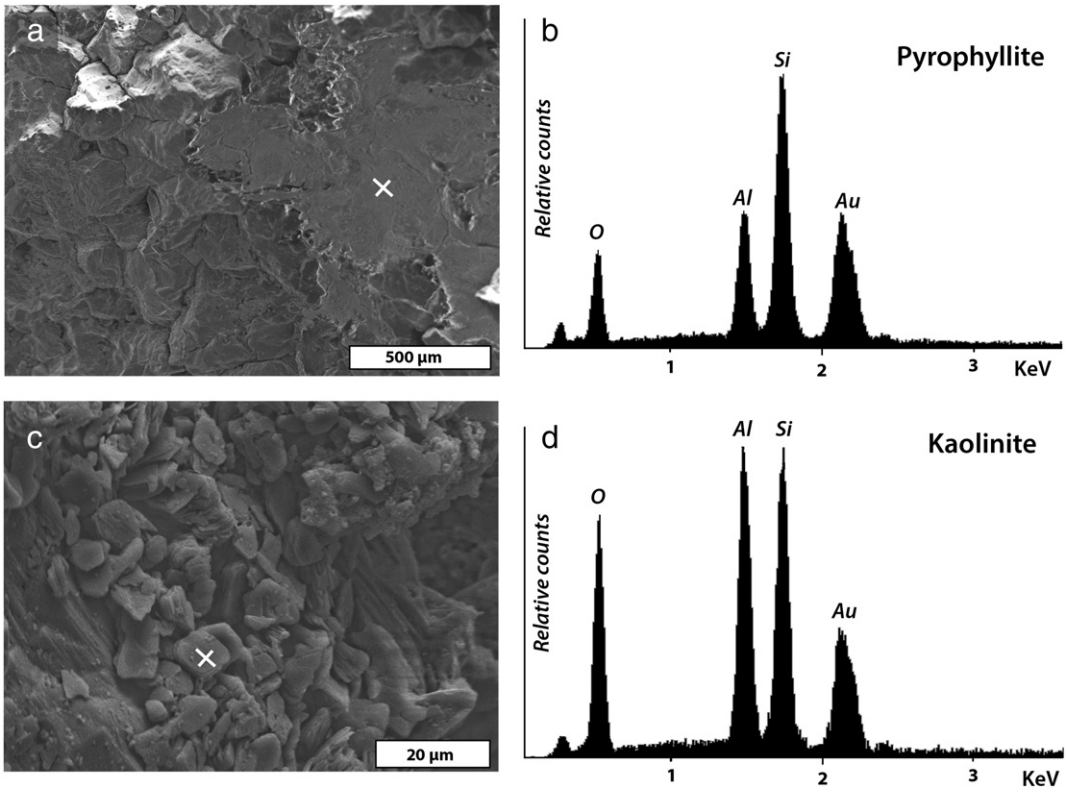

Fig. 7. SEM images and point-based EDAX analyses of pyrophyllite and kaolinite: a) fan-shaped plates of pyrophyllite filling pores between quartz grains; b) the EDAX counts on the cross shown in "a" reveal a ratio between silica and aluminium, Si/Al = 2 characterising pyrophyllite; c) pseudo-hexagonal clusters of plates of kaolinite covering quartz grains; and d) the EDAX counts of aluminium on the kaolinite clusters (cross in "c") are almost the same to silica because of the chemical ratio Si/Al = 1.

(producing also illite) were found to be active in the exhumation and weathering history of the phyllosilicate-rich quartz–sandstone of the Varanger Peninsula in northern Norway (Fjellanger and Nystuen, 2007).

5.3. Morphometry of pillar and mammillary features

The morphological measurements of pillars in Imawarì Yeuta cave are reported in Table 3. The data clearly show that the horizontal cross-section of the narrower central part of these columns is in most of cases an elongated ellipse rather than a circle. The length of the major axes (M) ranges between 10 and 130 cm, while the mean ellipticity e in the whole set of measurements is 1.9. Similar values of e are maintained, even considering different dimensional classes of major axes: 130 cm < e = 2.11 > 50 cm, 50 cm < e = 2.29 > 30 cm, 30 cm < e = 1.56 > 15 cm, and 15 cm < e = 1.63. Plotting the axis directions (ellipses) for each station of measurements in a rose diagram, it is shown that the pillars are characterised by specific orientations, often at angles of 15°, 30° and 60° between them (Fig. 10). In the majority of cases at each station these ellipses are not oriented along the stream flow direction, so they cannot be interpreted as the result of mere directional mechanical erosion. Conversely, with respect to the fracture sets documented at each station (red lines in Fig. 10), the major axes of the ellipses are oriented at 10–15° from the main fracture directions or approaching the bisector between the major conjugate sets. Furthermore, only 15% of the measured pillars are vertical while the majority of them are inclined, from only a few degrees up to 50°. In many cases specific inclinations are clearly related to fracture sets with the same dip (Fig. 11a–b) and characterise large groups of pillars in the same area. In addition, pillars are often in line with septums oriented parallel to evident major fractures (Fig. 11c).

Another documented morphology is the splitting of pillars in two or even more branches often with different inclinations (Fig. 11d–e). In most of the cases these splittings are related to secondary fractures observable at the junction (Fig. 11d arrow).

The morphometric analysis of the mammillary morphologies (or pendants) on the ceilings and floor of the cave passages shows almost the same relationship with the fracture sets (Fig. 12). Each pendant is delimited by a complex network of conjugate fractures and the associated ellipse's major axes result at 10–15° from the close related fracture or approach the bisector between the conjugate sets.

Table 2
Primary porosity of unweathered samples of quartz sandstones.

Sample	Direction	Por. %	Tepui	Description
R1	Perp.	4.64	Roraima	*Fresh almost pure quartz sandstone* with
	Parallel	6.98		cross bedding
GS7	Perp.	3.41	Auyan	*Fresh almost pure quartz sandstone* with
	Parall.	7.69		parallel bedding
AKT	Perp.	6.53	Akopan	*Slightly weathered almost pure quartz*
	Parall.	11.11		*sandstone* with cross bedding
IY11	Perp.	6.85	Auyan	*Slightly weathered almost pure quartz*
	Parall.	10.33		*sandstone* with cross bedding
IY10	Perp.	0.58	Auyan	*Fresh phyllosilicate-rich quartz sandstone*
	Parall.	0.24		with parallel bedding

6. Discussion

6.1. Strata-bounded fractures: the origin of pillars and maze network caves

Along the cliffs delimiting many of the secondary platforms in the Roraima, Auyan and Chimanta Tepuis, a repetition of hard beds forming overhanging and protruding strata and more fractured carved ones often characterised by half-pillar morphologies is evident (Fig. 13 but see also Fig. 47–48 in Aubrecht et al., 2012). These second

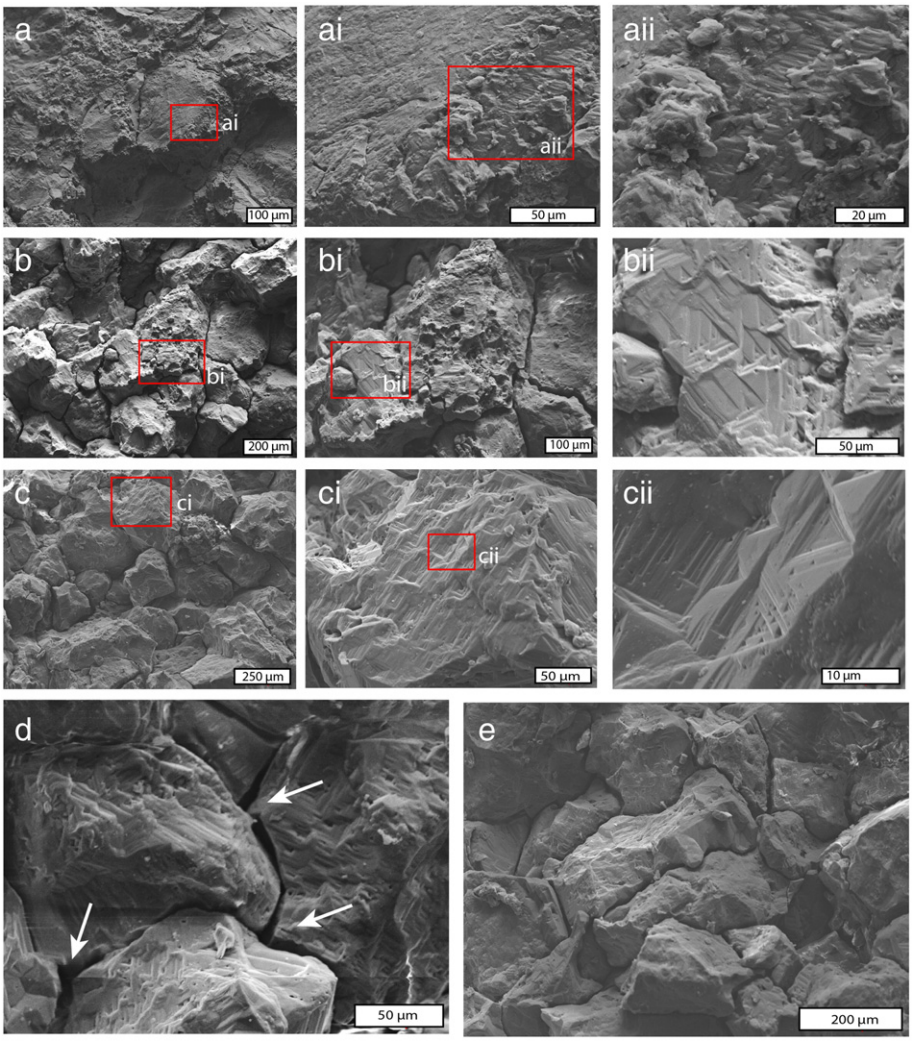

Fig. 8. SEM images of quartz–sandstone samples with different degree of cohesiveness: a) cohesive sample with abundant welding between the grains and by a pervasive syntaxial quartz overgrowth: at low magnification there are no evident signs of dissolution while at increasing magnification it is possible to observe small dissolution features starting to affect the grain surface (ai, aii); b) low cohesiveness samples showing a high porosity between the quartz grains that are clearly characterised by dissolution morphologies such as pitting (bi) and v-shapes (bii); c) almost non-cohesive sample with high intergranular porosity: all the grain surfaces are characterised by diffuse v-shaped dissolution features; d) highly weathered sample showing higher dissolution porosity at the triple junctions between quartz overgrowths: note the diffuse dissolution features on the whole surface of the grains; and e) highly weathered sample showing how the quartz grains are gradually released from the interlocked structure.

strata are frequently characterised by honeycomb features appearing to be more prone to weathering than the overlying and underlying protruding beds (Fig. 13a). The same situation is present also inside the caves, where the passages are often developed along specific strata where pillars are frequently formed, while roofs and floors are represented by massive and less fractured strata.

Previous authors (Aubrecht et al., 2008, 2011, 2013) interpreted this alternation of soft and harder beds as "purely diagenetic", i.e. due to an inhomogeneous diffusion of late diagenetic fluids through intergranular voids, related to the different hydraulic conductivity between coarse- and fine-grained sands. The funnel pillar morphologies would be related to the migration of these diagenetic fluids through delimited channels

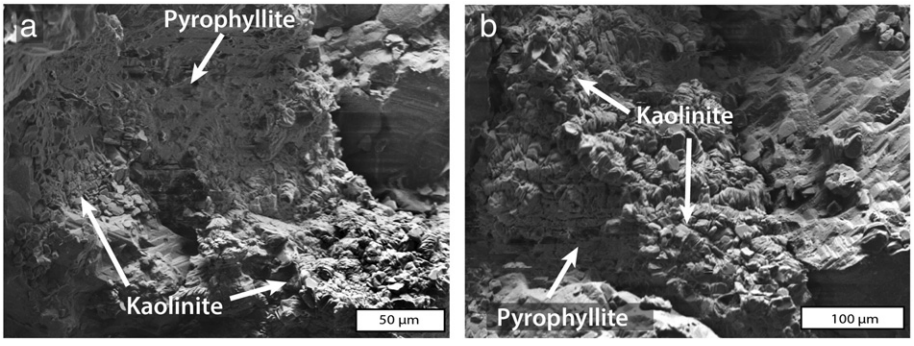

Fig. 9. a) Neo-forming kaolinite at the expenses of pyrophyllite through the dissolution recrystallization reaction described by Hurst and Könkle (1985): this reaction increases the porosity of the rock and favours access of water and dissolution of quartz: note the highly corroded quartz grain surface on the right in b).

Table 3
Morphological measurements of funnel-shape pillars in Imawarì Yeuta divided in measurement stations.

	M	m	D	i	id	M	m	D	i	id
Galeria Mil Columnas at point 53	25	15	273	−63	357	55	19	247	−61	159
	35	21	172	−74	91	70	38	244	−55	146
	22	18	187	−65	6	14	10	269	−75	14
	14	14	/	−79	104	20	10	173	−15	138
	70	47	100	−57	4	23	14	270	−90	/
	35	24	95	−65	3	29	24	256	−90	/
	21	13	90	−65	13	28	20	250	−90	/
	8	8	/	−67	7	58	40	260	−64	166
	15	8	29	−66	18	35	23	270	−71	172
	13	8	256	−81	20	42	15	200	−80	216
	30	13	76	−59	102	31	18	290	−62	218
Rio de los Venezuelanos at points S2–S4	27	80	261	−69	169	26	20	250	−79	314
	10	20	252	−70	183	70	30	226	−71	155
	37	15	240	−76	210	33	12	266	−84	332
	13	8	260	−75	199	35	24	250	−80	145
	7	5	232	−72	185	40	21	245	−80	210
	35	18	244	−72	183	25	29	262	−73	223
	37	20	261	−73	146	52	36	243	−75	185
	22	14	251	−82	202	25	20	234	−72	222
	23	20	295	−74	238	14	9	246	−76	185
	16	7	246	−77	339	22	10	221	−81	218
	34	16	259	−90	/	20	30	256	−82	190
	19	7	218	−77	277	40	25	217	−72	286
	15	8	195	−78	259	44	24	253	−77	221
	12	5	253	−75	317					
Rio de los Italianos at point 33	75	30	228	90	/	35	6	280	−67	191
	60	25	237	90	/	37	12	290	−57	204
	30	22	260	90	/	21	17	315	−58	225
	32	15	224	90	/	25	22	280	−73	171
	20	13	266	90	/	7	6	280	−60	159
	33	17	275	−70	7	43	20	263	−69	175
	38	25	258	−75	350	35	20	220	−72	114
	130	40	280	90	/	37	21	267	−80	149
	130	60	290	90	/	54	26	270	−83	277
Galeria Mil Columnas at point 65–71	54	26	358	−83	91	30	16	292	−73	168
	22	11	357	−83	334	38	25	165	−83	352
	24	11	0	−70	266	18	14	319	−76	46
	31	5	1	−79	263	28	18	244	−74	173
	50	26	350	−74	344	30	28	252	−90	/
	32	5	357	−73	215	19	18	252	−90	/
	24	12	320	−67	298	70	26	279	−90	/
	20	15	67	−64	318	15	8	316	−90	/
	16	9	11	−77	81	10	9	280	−77	198
	39	20	19	−68	119	25	17	36	−73	321
	25	11	49	−90	/	22	12	44	−59	320
	19	10	93	−90	/	28	15	193	−71	225
	11	6	21	−82	240	20	17	97	−78	235
	21	9	12	−90	/	15	10	199	−48	24
	70	42	196	−90	/	27	16	123	−67	221
	36	15	10	−90	/	20	16	111	−79	205
	10	4	14	−90	/	30	17	120	−72	210
	30	26	280	−61	180	16	13	89	−72	303
	62	38	280	−90	/	10	13	329	−79	303

in the form of “finger flows”. Therefore, for these authors, half-pillars would represent the harder lithified parts while the surrounding softer rock would have remained unlithified, and would have thus been readily removed by erosion because of its softness.

Conversely, the results presented in this paper point to a different interpretation where the density-spacing of fractures and the primary porosity of the different strata are the main factors controlling the intensity and distribution of the arenisation process driving the formation of pillar morphologies and horizontal caves in specific stratigraphic positions. Strata-bound intense fracturing is typical of alternating strata with different petrographic and rheological characteristics. These fractures can be related to regional stresses distributed along strata with different thickness (Pollard and Segall, 1987), or to local fluid overpressure during diagenesis (hydro-fracturation; Gudmundsson and Brenner, 2001; Brenner and Gudmundsson, 2004; Philipp et al., 2006). Joint spacing, aperture variations and arrest depend primarily on the mechanical properties of the host rock and on the strata thickness (Shackleton et al., 2005). If the stratigraphic sequence is composed of an alternation of anisotropic banks with different composition, and therefore a different Young's modulus, fractures can develop mainly along specific strata while others arrest or limit their propagation (Brenner and Gudmundsson, 2004). The coexistence of strata-bounded joints and less continuous fractures cutting all the strata can be the response of different stress regimes through time. While continuous fractures are connected vertically to the surface, strata-bounded fractures form networks that are interconnected mainly horizontally.

The chemical and petrographical analyses showed that in the studied cases the protruding homogeneous beds are composed mainly of phyllosilicate-rich quartz–sandstones, while the weathered, highly fractured strata are almost pure quartz–sandstones. This difference in composition, and therefore in mechanical properties, resulted in the development of the densely spaced fractures, mainly in the latter, pure

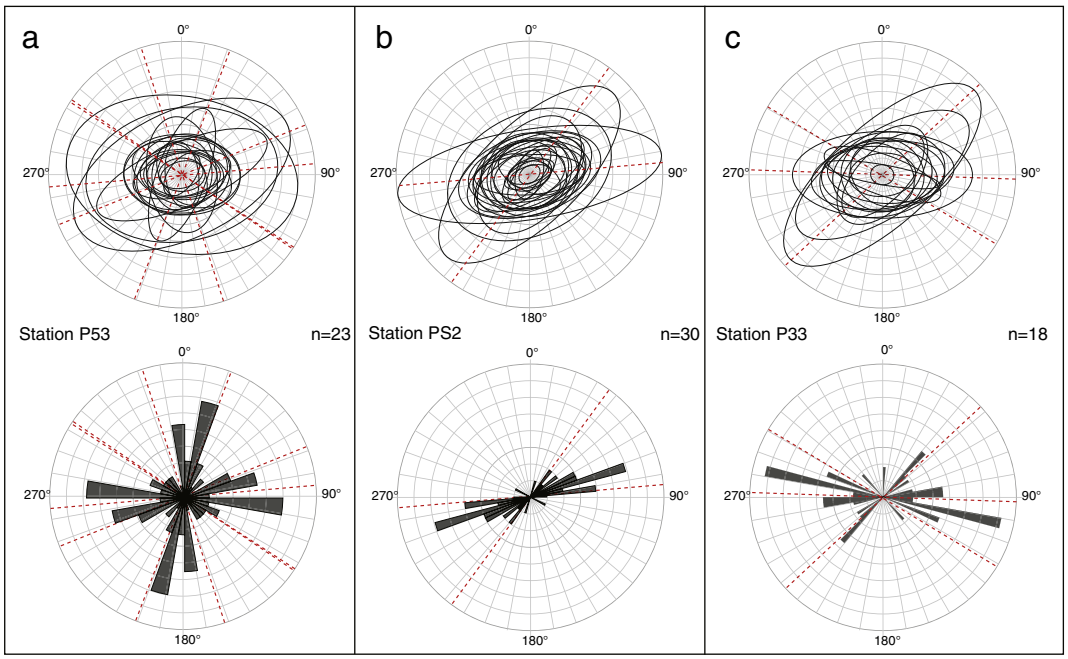

Fig. 10. Major and minor axes of the central pillar cross-section from three stations of measurements in Imawarì Yeuta cave: the major and minor axes are simplified as ellipses in the upper rose diagram, while the lower rose diagrams represent only the frequency of major axis directions and their relationship with the fracture set directions measured in the surroundings (red dotted lines).

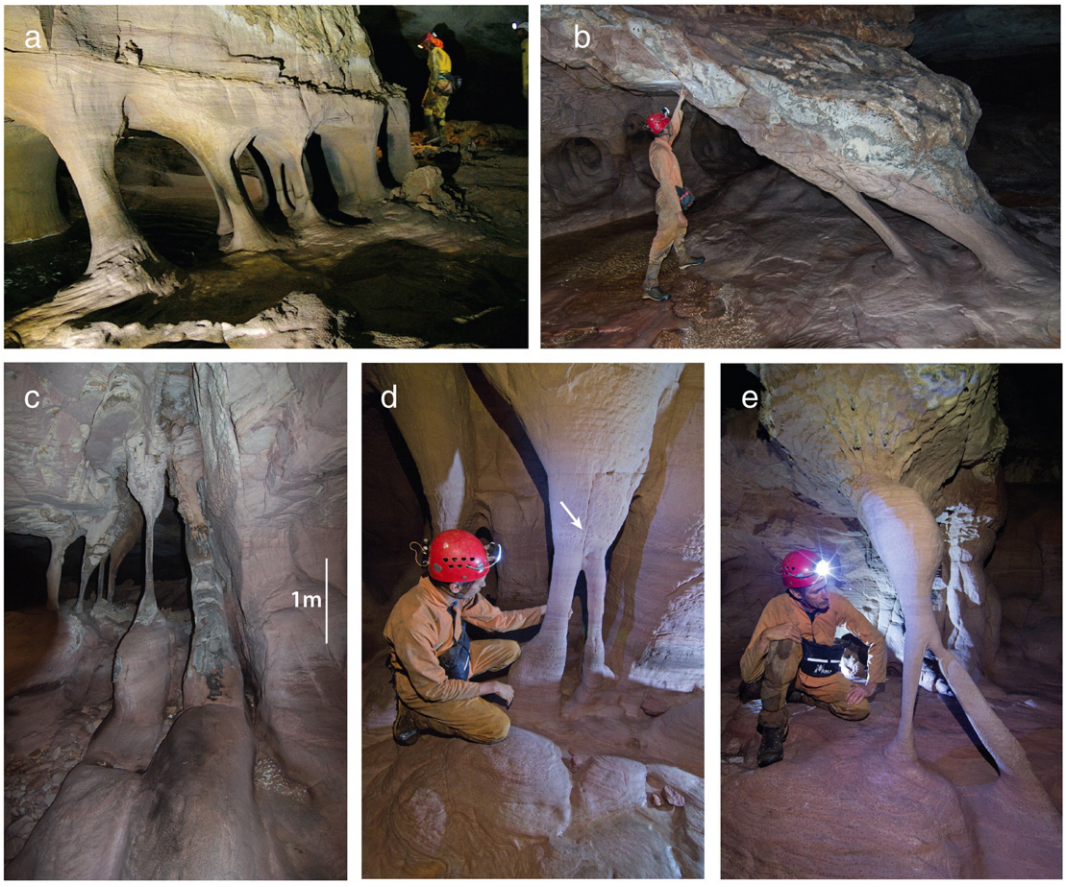

Fig. 11. Pillar morphologies related to local fracturing: a) set of aligned pillars inclined along local fractures; b) two highly inclined pillars evolved parallel to evident low angle fractures on the ceiling (above the speleologist); c) pillars formed along parallel fracture septums; d) Pillar splitting controlled by the enlargement of an evident vertical fracture (arrow); and e) pillar splitting in two differently inclined branches.

Fig. 12. Pendant morphologies protruding from the ceiling of Imawarì Yeuta cave: a) pendants are elongated, presenting an elliptical cross-section like the majority of the pillars; b) the relationship between pendants and the fracture network is evidenced in a zenital photo of the ceiling: the ellipses of the pendants develop mainly along the bisector of the conjugated fractures or along the secondary joint sets (see the rose diagram on the left).

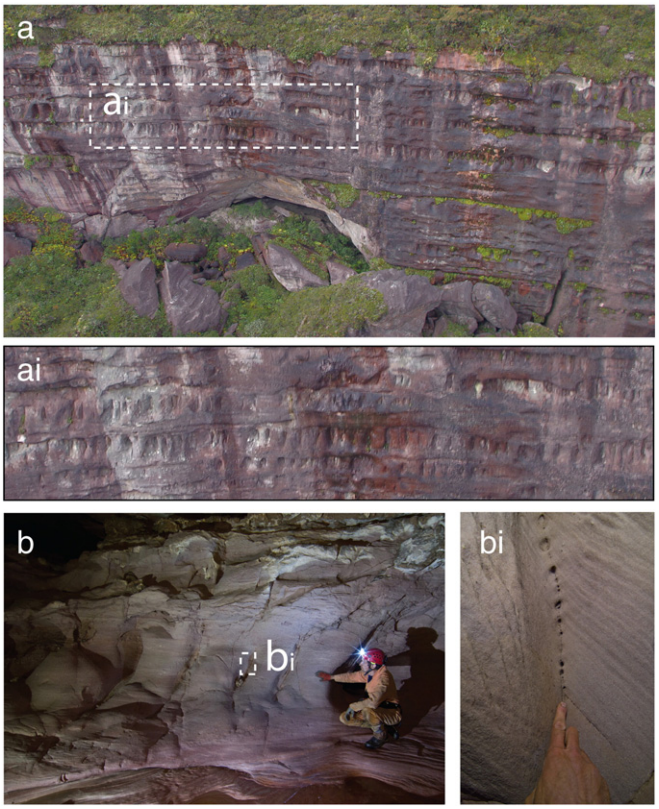

Fig. 13. Strata-bounded hydro-fractures: a) alternation of massive banks forming overhangings and denser fractured strata with half pillar morphologies on the cliff above the entrance "Sima del Viento" in Imawarì Yeuta cave: this regular alternation is clearly shown in ai; b) strata-bounded fractures along the cave walls: each fracture is wider in the central part and tapers away toward the overlying bed; bi) every fracture is clearly arenised and shows centimetric dissolution and piping tubes.
Photos from Francesco Sauro, La Venta.

quartz–sandstone strata. The evidence of these typical layer-bounded fractures is clearly found also in the cave walls (Fig. 13b), where joints become more inclined and thinner and finally taper away and come to arrest toward the overlying banks.

Such strata-bounded fracturing increases the surface area available for arenisation in these pure quartz–sandstone strata. When the undersaturated meteoric waters from the surface enter in this dense network of layer-bounded joints, dissolution initiates and propagates (Piccini and Mecchia, 2009). This process is effective even after hundreds of metres-long fracture pathways because of the extremely slow reaction kinetics of quartz dissolution allowing the water to remain undersaturated over long times and distances, causing arenisation of great volumes of rocks (Mecchia et al., 2014). Thus, arenisation works mainly underground along the more fractured layers, without necessary involving surface lowering. Some authors called this process in general "phantomisation" (Quinif, 1999; Häuselmann and Tognini, 2005; Dubois et al., 2014), because weathering predisposes the rock mass for the formation of caves that are afterward opened through piping and erosion.

The arenisation process is more effective in the almost pure quartz–sandstone mainly because of the following reasons:

- A higher primary porosity than the phyllosilicate-rich strata. A more porous sandstone displays a higher potential for the penetration of under-saturated water and for diffusion/dissolution transport between the quartz grains with subsequent deep weathering (Young, 1988; Wray, 1997b; Mecchia et al., 2014).
- The presence of a wide network of strata-bounded fractures that do not affect the phyllosilicate-rich strata. This complex macro- and microfracture system allows the penetration of under-saturated water in these strata, with consequent arenisation.
- Absence of residual clay minerals. In these strata the arenisation can work without producing residual clays like kaolinite that would clog the fractures and inhibit the process (Mecchia et al., 2014).

In the almost pure quartz–sandstone strata, the arenisation gradually decomposes the rock in between the existing fractures starting from the larger ones, or at the site where the initial aperture of these joints is wider, normally in the central part of the bed (Fig. 14). In a more advanced stage, the loose sand produced by weathering is removed by piping and the open fractures are gradually anastomosed, developing empty spaces between relict septa and pillars (Fig. 14c). The dimensions of this network and the presence of funnel-shaped pillars or wider massive remnants depend on the spacing between the fractures. The geometry of the weathering relics is easily predictable because these remnants will be aligned roughly along the major fracture sets or along rhombohedric conjugate joints (Fig. 14c). These relationships between joint families and pillars or pendants are clearly recognisable in the morphometric measurements reported from Imawarì Yeuta cave (Figs. 10–12). The final funnel and smooth shape of the pillars are probably related to both the propagation of the arenisation inside the pillar (Fig. 14f) and to the mechanism of "negative feedback" between stress and erosion in this type of sandstone morphologies, proposed recently by Bruthans et al. (2014).

The majority of the pillar fields are situated in the low, frequently flooded, areas of the cave probably because during flood events the

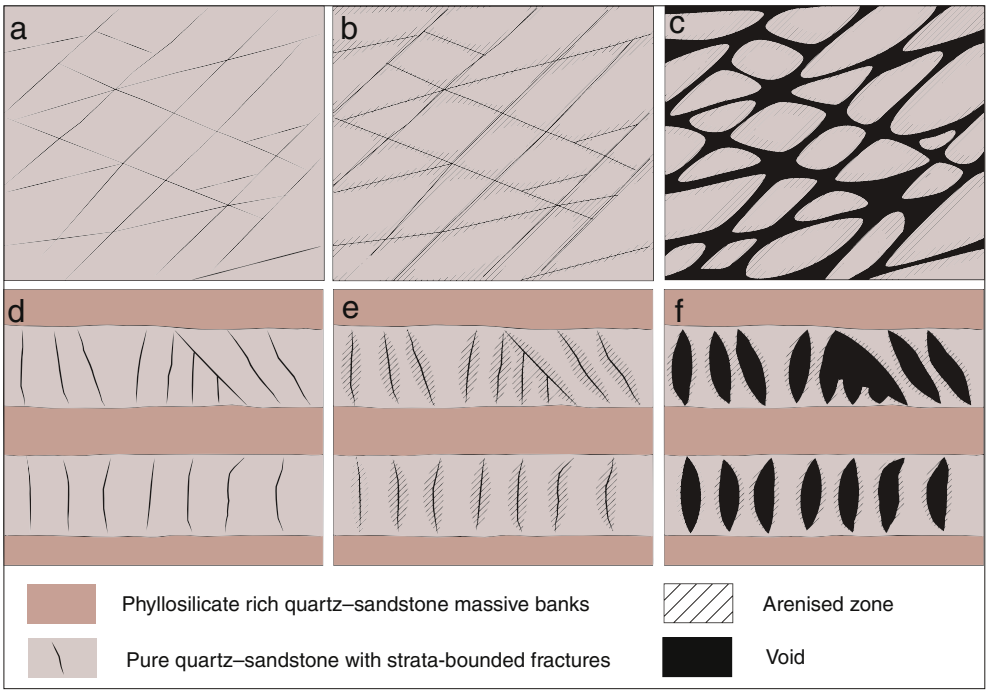

Fig. 14. Schematic model of the anastomosis of strata-bounded fractures through the arenisation process. In plan view: a) the fractured stratum is represented by a set of major and minor conjugate joints; b) arenisation propagates into the fractures being more intense at fracture intersections; and c) piping removes the loose sand produced by the arenisation process and frees the pillar morphologies that show a rhombohedral elliptic cross-section because of the fracture network geometry and of the enhanced arenisation at the fracture intersections. In vertical view: d) The fracture network is bounded in the almost pure quartz–sandstone layers, with the fracture aperture more prominent in the middle of the bed tapering away approaching the surrounding phyllosilicate-rich beds; e) arenisation propagates, starting and being more effective where the fracture aperture is wider in the middle of the bed; and f) piping removes the loose sand produced by the arenisation process and frees the funnel-shaped pillars that continue to be arenised during seasonal floods and by surface films of water due to condensation processes.

floodwater injection (Palmer, 2007) of highly under-saturated water on the cave sidewalls further propagates the arenisation process into the fractured strata. The floodwater injection process is particularly effective in the main underground streams that often form extremely wide meanders whose convex side is characterised by the most spectacular pillar morphologies (Sauro et al., 2013b). Clear examples of these settings in surface conditions are the sinkhole of El Foso (Fig. 15) and the closed depression of Lake Gladis in Roraima Tepui, whose flooded sidewalls are also characterised by well-developed pillar morphologies, as observed also by Aubrecht et al. (2012; Fig. 54). However pillar morphologies develop only when the fractures are densely spaced, otherwise if weathering propagates along few sets and major fractures, a main conduit or branchwork pattern develops. This is the case of Akopan Dal Cin and Guacamaya cave systems, with rectilinear corridors and rare or absent pillar morphologies.

Fig. 15. The effect of floodwater injection along strata-bounded fractures is evident in the sink of El Foso in the Roraima Tepui: the sidewalls of the cavity remain flooded for most of the year, showing well developed pillar morphologies.
Photo from Vittorio Crobu, La Venta Geographical Explorations Team.

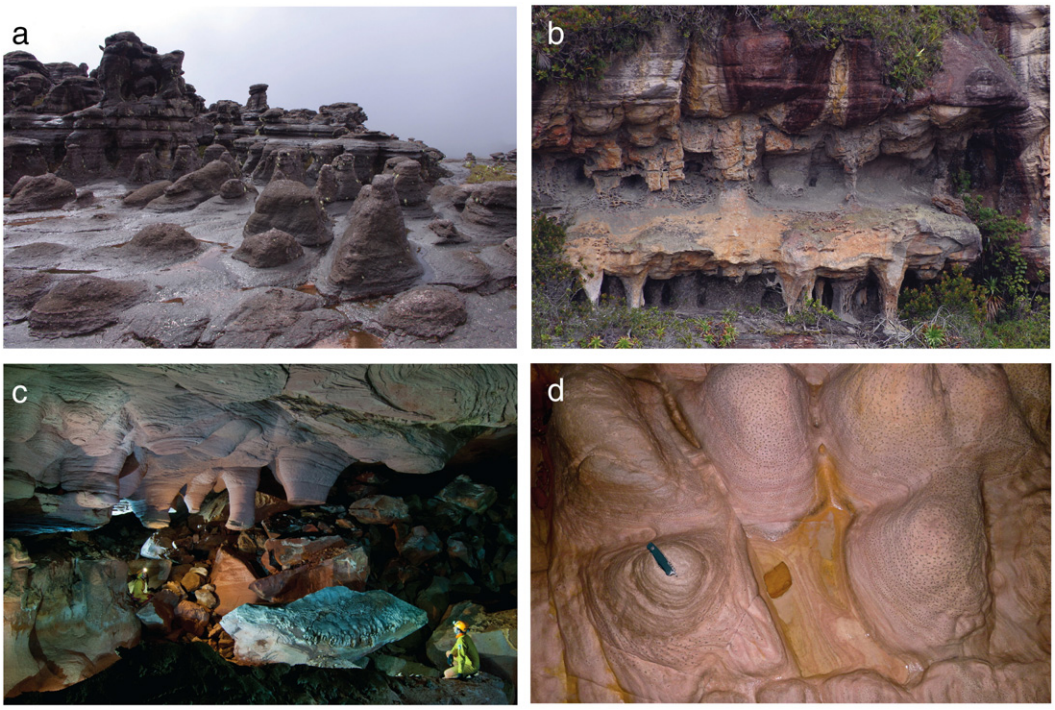

Fig. 16. Different morphologies resulting from arenisation along strata-bounded fracture networks. a) when a strata-bounded fracture network is open to the surface wide field of towers and pseudo-hexagonal or elliptic bumps develop on the platform surface (Roraima); b) half pillars develop on vertical walls; c) pendants and d) bumps develop on cave ceilings and floors in Imawarì Yeuta.
Photo from Vittorio Crobu, La Venta Geographical Explorations Team.

Arenisation can be active also along continuous fractures cutting the entire stratigraphic sequence, guiding the formation of vertical caves like the Aonda and Auyan Tepui Noroeste systems. In this case deep elongated narrow shafts develop along few fracture sets, often open by dilational gravitative stresses along the tepui rims. At the bottom or along these crevices, pillars and other similar morphologies are very rare, while long corridors are interconnected and septums are the result of anastomosing along parallel fractures.

In general, the loose sand produced by the arenisation process is accumulated in specific sectors of the systems, such in the inner side of meanders, low areas and rooms on the lateral side of active streams. However, the release of sand through arenisation has a much slower rate than the transport potential of the streams during flood events. Therefore, most of the loose sand produced is easily transported out of the system to the tepui surface and then to the lowlands surrounding the plateaus.

6.2. Stratigraphic guidance: the inception hypothesis in quartz–sandstones

As proposed by Martini (1985), arenisation is promoted mainly by under-saturated water seeping in fractures. When the fracture network

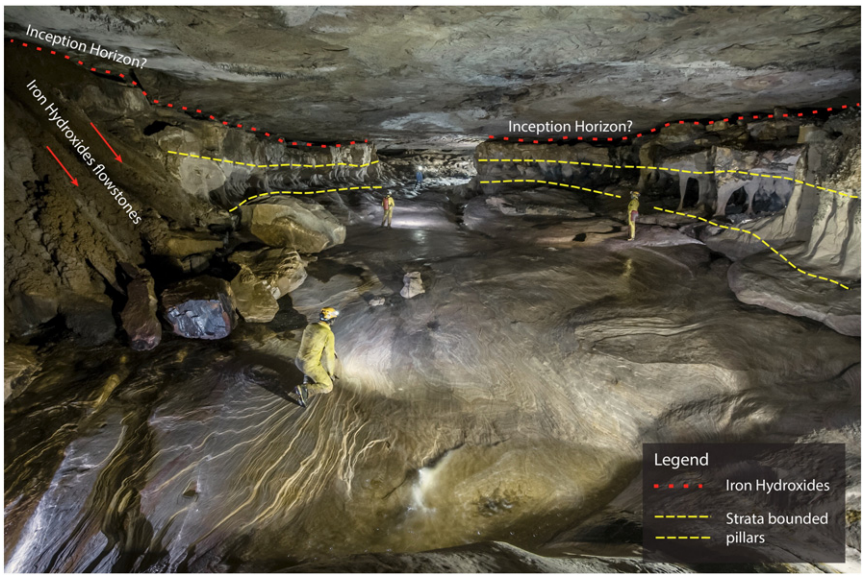

Fig. 17. Typical active gallery in Imawarì Yeuta: the open strata close to the ceiling is characterised by a layer of iron hydroxides, representing a prominent inception horizon; the iron hydroxides flow plastically or are deposited by seeping waters as flowstones on the side walls of the conduits; strata-bounded columns characterise the side walls of the conduit.
Photo: Alessio Romeo, La Venta Geographical Explorations Team.

is layer-bounded, as in the case described for Imawarì Yeuta, water can penetrate from the surface only when the stratum is uncovered by surface lowering, or dissected by secondary continuous fractures or scarp retreat. If one of these strata is unroofed on the plateau surface, spectacular fields of towers develop (Fig. 16a). When the strata is dissected laterally by secondary continuous fractures due to gravitational release or collapses along the cliffs, half pillars and honeycomb features alternating with overhanging massive banks develop on these vertical walls (Fig. 12a–b; Fig. 16b). Conversely, only in the presence of some specific layers or continuous fractures conveying the water flow into the subsurface specifically along a dense fractured stratum, arenisation is able to predispose the development of extensive horizontal strata-bounded cave systems with typical pillars, pendants and floor bumps (Fig. 16c–d).

In carbonate rocks the layers particularly favourable for the development of the primary cave conduits were debated in the Inception Horizon Hypothesis (IHH) proposed by Lowe (1992) and then investigated in detail by Filipponi et al. (2009). Applying their definition to the quartz–sandstone environment, we can assert that here the inception horizons could be "layers especially favourable to the opening of proto-conduits through karstic or weathering processes by virtue of physical, lithological or chemical deviation from the predominant quartz–sandstone facies" (Sauro et al., 2013c). Therefore we have to verify the presence of some specific layers along which the cave system develops, other than solely fractured beds that are common in the stratigraphic sequence.

In the majority of the investigated caves speleologists noticed the presence of residual deposits or continuous layers of iron hydroxides (mainly goethite; Sauro et al., 2014) guiding the gallery passages like those described in the Guacamaya cave, Akopan-Dal Cin and Imawarì Yeuta cave systems (Sauro et al., 2013d). These layers are often difficult to identify, being more easily weathered than the surrounding quartz–sandstones. In Guacamaya cave the iron hydroxide beds have all the characteristics of a Banded Iron Formation, locally folded and stretched because of shear related to the lithostatic load and the stronger rigidity of the overlying beds of quartz–sandstones (Sauro et al., 2013d). Also in Imawarì Yeuta it is possible to observe remnants of this hard iron-hydroxide strata (Fig. 17), almost with the same characteristics of the one described in Guacamaya cave. In addition, in all the studied caves it is possible to observe iron hydroxides plastically flowed, or deposited by seeping water, out from the main interstrata forming massive brownish flowstones, similar to other goethite speleothems described in other quartzite caves of the Sarisariñama and Chimanta Tepuis (Zawidzki et al., 1976; Aubrecht et al., 2011).

Reardon (1979) suggested that iron-silicate complexes (like Fe-H_2SiO_4) might increase the silicic acid solubility. This supposition was later confirmed by the studies of Morris and Fletcher (1987) and Serezhnikov (1989) showing that in ferrous iron solutions under oxidising conditions the potential solubility of quartz increases by a factor 10 over that of amorphous silica. Therefore, iron hydroxide layers located in only a few stratigraphic positions could have been favourable pathways for the formation of proto-conduits in local phreatic settings (Wray, 2009), promoting the infiltration of meteoric water in the surrounding fractured strata.

Moreover, also local layers of shales and silt could have been preferential infiltration pathways working either as aquicludes or as aquitards, allowing water to infiltrate along specific stratigraphic surfaces. Galán et al. (2004) noticed the presence of centimetre-thick layers of shale and siltstone guiding the development of the conduits in the Roraima Sur Cave System. Szczerban et al. (1977) described a horizontal cave system in the Guaiquinima Tepui whose development is clearly guided by siltstone layers. Similar lithological controls were described also by Piccini (1995) and Piccini and Mecchia (2009) in the Aonda and Auyan Tepui Noroeste fissure systems with thin layers of silts guiding the formation of major ledges along the walls of *simas* and controlling the horizontal collectors at the bottom of the shafts. In fact, gravitational release fractures along the peripheral rims could have also focused the water flow deep into the rock mass, concentrating at certain stratigraphic horizons that can work also as sliding surfaces during the dilation movements. These fractures represent true "tectonic inceptions" from which the development of a crevice-like cave system can start (Sauro et al., 2013a).

7. Conclusions

This study demonstrates that the arenisation process proposed by Martini (1979) and Jennings (1983) works with different intensities depending on the petrographical characteristics of the quartz–sandstone, being effective only where meteoric water can access the rock through specific stratigraphic or tectonic pathways. The effectiveness of the arenisation process in these strata is clearly demonstrated by SEM observations, with diffused pitting and V-shaped features on the quartz grains, typical of slow dissolution kinetics, and increasing porosities at the grain contacts.

Arenisation provides an effective explanation of all the morphologies found in the caves of the tepui massif. Pillars and pendants clearly represent the relics of weathering anastomosis between strata-bounded fractures and there is no need to invoke peculiar diagenetic conditions that do not seem to fit into the geologic history of the area, as proposed by Aubrecht et al. (2011, 2012).

The primary porosity and the degree of fracturing of the quartz–sandstone beds result as the main factors controlling the intensity and the distribution of the arenisation process, together with peculiar inception horizons. The formation of the giant anastomotic cave systems like Imawarì Yeuta or Roraima Sur is related to a combination of favourable conditions that include the presence of prominent inception horizons and dense strata-bounded fracturing.

While mechanisms other than true dissolution, such as piping and mechanical erosion, largely modelled the landscape and finally carved the caves of the tepui into the weathered rock, quartz dissolution evidently plays an essential and triggering role. Thus, these processes could be effectively considered as "true karst" as proposed by several authors (Wray, 2000, 2013; Young et al., 2009; Eberhard and Sharples, 2013).

Acknowledgements

I would like to thank Jo De Waele, Leonardo Piccini, Marco Mecchia and Paolo Forti for their suggestions and useful discussion on this topic. My gratitude goes also to Freddy Vergara and all the speleologists from the Theraphosa and La Venta exploring teams. Many thanks also to Nicola Tisato who performed the compositional and porosity analyses at the ETH of Zurich, to Ermanno Galli for the mineralogical analyses at the University of Modena and Reggio Emilia and to Giorgio Gasparotto and Enrico Dinelli for help in the SEM and WDS analyses at the University of Bologna.

This research has benefited from the permit for speleological research from the Instituto National de Parques (INParques) and the patronage of the Government of Bolivar State from Venezuela, and from the economic support of many sponsors: Geotec S.P.A., Dolomite, Intermatica, Ferrino, Napapijri, and Allemano Metrology. Many thanks also to Tiziano Conte who supported the 2014 expedition. The researches conducted by the author on the tepui table mountains are supported by the Rolex Award for Enterprise Program.

References

Aubrecht, R., Lánczos, T., Šmída, B., Brewer-Carías, Ch., Mayoral, F., Schlögl, J., Audy, M., Vlček, L., Kováčik, Ľ., Gregor, M., 2008. Venezuelan sandstone caves: a new view on their genesis, hydrogeology and speleothems. Geol. Croat. 61, 345–362.

Aubrecht, R., Lánczos, T., Gregor, M., Schlögl, J., Šmída, B., Brewer-Carías, Ch., Vlček, L., 2011. Sandstone caves on Venezuelan tepuis: return to pseudokarst? Geomorphology 132, 351–365.

Aubrecht, R., Barrio-Amorós, C.L., Breure, A.S.H., Brewer-Carías, C., Derka, T., Fuentes-Ramos, O.A., Gregor, M., Kodada, J., Kováčik, Ľ., Lánczos, T., Lee, N.M., Liščák, P., Schlögl, J., Šmída, B., Vlček, L., 2012. Venezuelan tepuis: their caves and biota. Acta Geologica Slovaca MonographComenius University, Bratislava, (168 pp.).
Aubrecht, R., Lánczos, T., Gregor, M., Schlögl, J., Šmída, B., Liščák, P., Brewer-Carías, Ch., Vlček, L., 2013. Reply to the comment on "Sandstone caves on Venezuelan tepuis: return to pseudokarst?". Geomorphology 197, 197–202.
Audy, M., Bouda, R., 2013. Quartz–sandstone caves on table mountains of Venezuela. In: Filippi, M., Bosak, P. (Eds.), Proceedings of the 16th International Congress of Speleology, Brno 19–27 July 2013. Vol. 2, pp. 20–23.
Barton, H., Suarez, P., Muench, B., Giarrizzo, J., Broering, M., Banks, E., Venkateswaran, K., 2009. The alkali speleogenesis of Roraima Sur Cave, Venezuela. In: White, W.B. (Ed.), Proceedings of the 15th International Congress of Speleology, Kerrville, Texas, 19–26 July 2009, pp. 802–807.
Bernabei, T., Mecchia, M., Pezzolato, P., Piccini, L., Preziosi, E., 1993. Tepuy'93: ancora Venezuela! Speleologia 29, 8–23.
Brenner, S.L., Gudmundsson, A., 2004. Arrest and aperture variation of hydrofractures in layered reservoirs. Geol. Soc. Lond. Spec. Publ. 231 (1), 117–128.
Brewer-Carías, C., Audy, M., 2011. Entrañas del mundo perdido. Corpo Print (Ed), Caracas, (290 pp).
Briceño, H.O., Schubert, C., 1990. Geomorphology of the Gran Sabana, Guyana Shield, southeastern Venezuela. Geomorphology 3, 125–141.
Bruthans, J., Soukup, J., Vaculikova, J., Filippi, M., Schweigstillova, J., Mayo, A.L., Masin, D., Kletetschka, G., Rihosek, J., 2014. Sandstone landforms shaped by negative feedback between stress and erosion. Nat. Geosci. http://dx.doi.org/10.1038/ngeo2209.
Burley, S.D., Kantorowicz, J.D., 1986. Thin section and S.E.M. textural criteria for the recognition of cement-dissolution porosity in sandstones. Sedimentology 33, 587–604.
Carreño, R., Nolla, J., Astort, J., 2002. Cavidades del Wei-Assipu Tepui, Macizo del Roraima, Brasil. Bol. Soc. Venez. Espeleol. 36, 36–45.
Chalcraft, D., Pye, K., 1984. Humid tropical weathering of quartzite in southeastern Venezuela. Z. Geomorphol. 28, 321–332.
Doerr, S.H., 1999. Karst-like landforms and hydrology in quartzites of the Venezuelan Guyana shield: pseudokarst or "real" karst? Z. Geomorphol. 43, 1–17.
Dubois, C., Quinif, Y., Baele, J.-M., Barriquand, L., Bini, A., Bruxelles, L., Dandurand, G., Havron, C., Kaufmann, O., Lans, B., Maire, R., Martin, J., Rodet, J., Rowberry, M.D., Tognini, P., Vergari, A., 2014. The process of ghost-rock karstification and its role in the formation of cave systems. Earth Sci. Rev. 131, 116–148.
Eberhard, R.S., Sharples, C., 2013. Appropriate terminology for karst-like phenomena: the problem with 'pseudokarst'. Int. J. Speleol. 42 (2), 109–113.
Filipponi, M., Jeannin, P., Tacher, L., 2009. Evidence of inception horizons in karst conduit networks. Geomorphology 106, 86–99.
Fjellanger, J., Nystuen, J.P., 2007. Diagenesis and weathering of quartzite at the palaeic surface on the Varanger Peninsula, northern Norway. Nor. J. Geol. 87 (1/2), 239–251.
Franzini, M., Leoni, L., Saitta, M., 1972. A simple method to evaluate the matrix effects in X-ray fluorescence analysis. X-Ray Spectrom. 1, 151–154.
Galán, C., 1991. Expedición SVE a los tepuys Ilù, Tramen y Iuruaní. Bol. Soc. Venez. Espeleol. 25, 47.
Galán, C., 1992. El clima del macizo del Chimantá. In: Huber, O. (Ed.), El Macizo del Chimantá – Escudo della Guayana, Venezuela – Un ensayo ecologico tepuyano. O. Todtman Editors, Caracas, pp. 37-52.
Galán, C., Lagarde, J., 1988. Morphologie et evolution des cavernes et formes superficielles dans les quartzites du Roraima. Karstologia 11–12, 49–60.
Galán, C., Herrera, F.F., Carreño, R., 2004. Geomorfología e hidrología del Sistema Roraima Sur, Venezuela, la mayor cavidad del mundo en cuarcitas: 10,8 km. Bol. Soc. Venez. Espeleol. 38, 2–16.
Ghosh, S.K., 1985. Geology of the Roraima Group and its implication. Boletin de Geologia, Venezuela, Pub. Especial. 10, pp. 33–50.
Gibbs, A.K., Barron, C.N., 1993. The Geology of the Guyana Shield. Clarendon Press, Oxford, (246 pp.).
González de Juana, C., Picard, X., Iturralde, J.M., 1980. Geologia de Venezuela y de sus cuencas petrolifera. Edic. Foninves, Caracas, (1031 pp.).
Gori, S., Inglese, M., Tognini, P., Trezzi, G., Rigamonti, I., 1993. Auyan-tepui, speleologia tropicale nelle quarziti. Speleologia 28, 23–33.
Gratier, J., Muquet, L., Hassani, R., Renard, F., 2005. Experimental microstylolites in quartz and modeled application to natural stylolitic structures. J. Struct. Geol. 27, 89–100.
Gudmundsson, A., Brenner, S.L., 2001. How hydrofractures become arrested. Terra Nova 13 (6), 456–462.
Hartikainen, K., Hautojärvi, A., Kuoppamäki, K., Timonen, J., 1996. Helium gas methods for rock characteristics and matrix diffusion. In: Posiva (Ed.), Helsinki, Report Number 96-22 (58 pp.).
Häuselmann, P., Tognini, P., 2005. Kaltbach cave (Siebenhengste, Switzerland): phantom of the sandstone? Acta Carsol. 34 (2), 383–396.
Hawkes, D.D., 1966. Differentiation of the Tumatumari–Kopinang dolerite intrusion, British Guiana. Geol. Soc. Am. Bull. 77 (10), 1131–1158.
Hurst, V.J., Könkle, A.C., 1985. Dehydroxylation, rehydroxylation, and stability of kaolinite. Clay Clay Miner. 33, 1–14.
Ipiña, J.M., 1994. Aspectos físico-químicos de los tepuyes Acopan y Amuri. Macizo de Chimanta, Gran Sabana, Venezuela. Bol. Soc. Venez. Espeleol. 28, 5–9.
Jennings, J.N., 1983. Sandstone pseudokarst or karst? In: Young, R.W., Nanson, G.C. (Eds.), Aspects of Australian Sandstone Landscape. Australia and New Zealand Geomorphology Group Special Publication, Wollongong, pp. 21–30.
Leoni, L., Saitta, M., 1976. X-ray fluorescence analysis of 29 trace elements in rock and mineral standards. Rend. Soc. Ital. Mineral. Petrol. 32, 497–510.
Leoni, L., Menichini, M., Saitta, M., 1982. Determination of S, Cl, and F in silicate rocks by X-ray fluorescence analyses. X-Ray Spectrom. 11, 156–158.
Lowe, D.J., 1992. The Origin of Limestone Caverns: An Inception Horizon Hypothesis. (Ph.D. thesis) Manchester Metropolitan University, (512 pp.).
Marker, M.E., 1976. Note on some South African pseudokarst. Bol. Soc. Venez. Espeleol. 7 (13), 5–12.
Martini, J.E.J., 1979. Karst in black reef quartzite near Kaapsehoop, eastern Transvaal. Ann. S. Afr. Geol. Surv. 13, 115–128.
Martini, J.E.J., 1985. Les phénomènes karstiques de quartzites d'Afrique du Sud. Karstologia 9, 45–52.
Martini, J.E.J., 2000. Dissolution of quartz and silicate minerals. In: Klimchouk, A.B., Ford, D.C., Palmer, A.N., Dreybrodt, W. (Eds.), Speleogenesis: Evolution of Karst Aquifers. National Speleological Society, Huntsville, pp. 452–457.
Martini, J.E.J., 2004. Silicate karst. In: Gunn, J. (Ed.), Encyclopedia of Caves and Karst Science. Fitzroy Dearborn, London, pp. 1385–1393.
Mecchia, M., Piccini, L., 1999. Hydrogeology and SiO_2 geochemistry of the Aonda Cave system (Auyantepui, Bolivar, Venezuela). Bol. Soc. Venez. Espeleol. 33, 1–11.
Mecchia, M., Sauro, F., Corongiu, C., Crobu, V., 2009. Speleological explorations in the Chimanta massif quartzites (Gran Sabana, Venezuela). Supplement to Kur Magazine. 12, (16 pp.).
Mecchia, M., Sauro, F., Piccini, L., De Waele, J., Sanna, L., Tisato, N., Lira, J., Vergara, F., 2014. Geochemistry of surface and subsurface waters in quartz–sandstones: significance for the geomorphic evolution of tepui table mountains (Gran Sabana, Venezuela). J. Hydrol. 511, 117–138.
Morris, R.C., Fletcher, A.B., 1987. Increased solubility of quartz following ferrous–ferric iron reactions. Nature 330, 558–561.
Palmer, A.N., 2007. Cave Geology. Cave Books, Dayton, OH, (454 pp.).
Philipp, S.L., Hoffmann, S., Bartelsen, T., Oelrich, A., Gudmundsson, A., 2006. Field studies and numerical models of hydrofracture propagation in mechanically layered rocks. Geophys. Res. Abstr. 8 (abstract number 06374).
Piccini, L., 1995. Karst in siliceous rocks — karst landforms and caves in the Auyàn-tepui massif (est. Bolivar, Venezuela). Int. J. Speleol. 24 (1–4), 41–54.
Piccini, L., Mecchia, M., 2009. Solution weathering rate and origin of karst landforms and caves in the quartzite of Auyan-tepui (Gran Sabana, Venezuela). Geomorphology 106, 15–25.
Pollard, D.D., Segall, P., 1987. Theoretical displacements and stresses near fractures in rock: with applications to faults, joints, veins, dikes, and solution surfaces. Fract. Mech. Rock 277 (349), 277–349.
Quinif, Y., 1999. Fantômisation, cryptoaltération et altération sur roche nue, le triptyque de la karstification. Etudes de géographie physique, suppl. XXVIII,pp. 159–164.
Reardon, E.J., 1979. Complexing of silica by iron (III) in natural waters. Chem. Geol. 25 (4), 339–345.
Reid, A.R., 1974. Stratigraphy of the type area of the Roraima Group, Venezuela. Bolletin de Geologia, Venezuela, Pub. Especial. 6, pp. 343–353.
Rigamonti, I., 1995. La roccia. Il Grottesco, Special Issue. ,pp. 32–40.
Santos, J.O.S., Potter, P.E., Reis, N.J., Hartmann, L.A., Fletcher, I.R., McNaughton, N.J., 2003. Age, source, and regional stratigraphy of the Roraima Supergroup and Roraima-like outliers in northern South America based on U–Pb geochronology. Geol. Soc. Am. Bull. 115, 331–348.
Sauro, F., 2009. Mondi Perduti, sugli altopiani quarzitici del Venezuela. Speleologia 61, 38–47.
Sauro, F., Zampieri, D., Filipponi, M., 2013a. Development of a deep karst system within a transpressional structure of the Dolomites in north-east Italy. Geomorphology 184, 51–63.
Sauro, F., De Vivo, A., Vergara, F., De Waele, J., 2013b. Imawarì Yeuta: a new giant cave system in the quartz–sandstones of the Auyan Tepui, Bolivar state, Venezuela. In: Filippi, M., Bosak, P. (Eds.), Proceedings of the 16th International Congress of Speleology, Brno 19–27 July 2013. vol. 2, pp. 142–146.
Sauro, F., Piccini, L., Mecchia, M., De Waele, J., 2013c. Comment on "Sandstone caves on Venezuelan tepuis: return to pseudokarst?" by R. Aubrecht, T. Lánczos, M. Gregor, J. Schlögl, B. Smída, P. Liscák, Ch. Brewer-Carías, L. Vlcek. Geomorphology 132, 351–365 (Geomorphology 197, 190–196).
Sauro, F., Lundberg, J., De Waele, J., Tisato, N., Galli, E., 2013d. Speleogenesis and speleothems of the Guacamaya Cave, Auyan Tepui, Venezuela. In: Filippi, M., Bosak, P. (Eds.), Proceedings of the 16th International Congress of Speleology, Brno 19–27 July 2013. vol. 3, pp. 298–304.
Sauro, F., Tisato, N., De Waele, J., Bernasconi, S., Bontognali, R.R.T., Galli, E., 2014. Source and genesis of sulphate and phosphate–sulphate minerals in quartz–sandstone cave environment. Sedimentology 61 (5), 1433–1451.
Serezhnikov, A.I., 1989. Silica in acid natural solutions. Transactions (Doklady) of the USSR Academy of Sciences, Earth Science Section. 298, pp. 134–138.
Shackleton, J.R., Cooke, M.L., Sussman, A.J., 2005. Evidence for temporally changing mechanical stratigraphy and effects on joint-network architecture. Geology 33 (2), 101–104.
Sloss, L.L., Feray, D.E., 1948. Microstylolites in sandstone. J. Sediment. Res. 18 (1), 3–13.
Sociedad Venezolana de Espeleologia, 1984. Catastro Espeleologico National. Bol. Soc. Venez. Espeleol. 22, 65–75.
Sociedad Venezolana de Espeleologia, 1994. Cavidades Estudiadas en la Expedición al Macizo de Chimanta, 1993. Bol. Soc. Venez. Espeleol. 28, 34–51.
Szczerban, E., Urbani, F., 1974. Formas carsicas en areniscas Precambricas del Territorio Federal Amazonas y Estado Bolivar. Bol. Soc. Venez. Espeleol. 5 (1), 25–54.
Szczerban, E., Urbani, F., Colveé, P., 1977. Cuevas y simas en cuarcitas y metalimolitas del Grupo Roraima, Meseta de Guaiquinima, Estado Bolivar. Bol. Soc. Venez. Espeleol. 8, 127–154.
Teggin, D., Martinez, M., Palacios, G., 1985. Un estudio preliminar de las diabasas del estado Bolivar, Venezuela. Memorias VI Congreso Geologico Venezolano, pp. 2159–2206 (Caracas).
Tricart, J., 1972. The Landforms of the Humid Tropics, Forests and Savannas. Longman, London, (306 pp.).

Urbani, F., Talukdar, S., Szczerban, E., Colveé, P., 1977. Metamorfismo de las rocas del Grupo Roraima. Edo. Bolívar y Territorio Federal Amazonas. Memorias V Congreso Geologico Venezolano, Caracas, pp. 623–638.
White, A.F., Peterson, M., 1990. The role of reactive surface areas in chemical weathering. Chem. Geol. 84, 334–336.
Wray, R.A.L., 1993. Solutional landforms on silicates; largely ignored or largely unrecognised? 19th Biennial Conference of the Australian Speleological Federation, Launceston (110 pp.).
Wray, R.A.L., 1997a. A global review of solutional weathering forms on quartz–sandstones. Earth Sci. Rev. 42, 137–160.
Wray, R.A.L., 1997b. Quartzite dissolution: karst or pseudokarst? Cave Karst Sci. 24, 81–86.
Wray, R.A.L., 2000. The Gran Sabana: the world's finest quartzite karst? In: Migon, P. (Ed.), Geomorphological Landscapes of the World. Springer, pp. 79–88.
Wray, R.A.L., 2009. Phreatic drainage conduits within quartz–sandstone: evidence from the Jurassic Precipice Sandstone, Carnarvon Range, Queensland, Australia. Geomorphology 110 (3), 203–211.
Wray, R.A.L., 2013. Solutional weathering and karstic landscapes on quartz sandstones and quartzite. In: Frumkin, A. (Ed.), Treatise on GeomporphologyKarst Geomorphology. vol. 6. Elsevier.
Young, R.W., 1988. Quartz etching and sandstone karst: examples from the East Kimberleys, Northwestern Australia. Z. Geomorphol. 32, 409–423.
Young, R.W., Wray, R.A.L., Young, A.R.M., 2009. Sandstone Landforms. Cambridge University Press, Cambridge, (314 pp.).
Zawidzki, P., Urbani, F., Koisar, B., 1976. Preliminary notes on the geology of the Sarisariñama plateau, Venezuela, and the origin of its caves. Bol. Soc. Venez. Espeleol. 7, 29–37.